BioMetals

Structural and solution chemistry, antiproliferative effects, and serum albumin binding of three pseudohalide derivatives of Auranofin

--Manuscript Draft--

Manuscript Number:	BIOM-D-19-00209
Full Title:	Structural and solution chemistry, antiproliferative effects, and serum albumin binding of three pseudohalide derivatives of Auranofin
Article Type:	Original
Keywords:	Metal Based Drugs; NMR; Cancer; Protein Metalation; BSA
Corresponding Author:	DAMIANO CIRRI Università degli Studi di Firenze Firenze, Toscana ITALY
Corresponding Author Secondary Information:	
Corresponding Author's Institution:	Università degli Studi di Firenze
Corresponding Author's Secondary Institution:	
First Author:	DAMIANO CIRRI
First Author Secondary Information:	
Order of Authors:	DAMIANO CIRRI
	Maria Giulia Fabbrini
	Lara Massai
	Serena Pillozzi
	Annalisa Guerri
	Alessio Menconi
	Luigi Messori
	Tiziano Marzo
	Alessandro Pratesi
Order of Authors Secondary Information:	
Funding Information:	AIRC (22294) — Dr. DAMIANO CIRRI
	Università di Pisa (Rating Ateneo 2018/2019) — Dr. Tiziano Marzo
	AIRC (19650) — Prof. Luigi Messori
	ECRF (19650) — Prof. Luigi Messori
Abstract:	Three pseudohalide analogues of the established gold drug Auranofin (AF hereafter), of general formula Au(PEt 3)X, i.e. Au(PEt 3)CN, Au(PEt 3)SCN and Au(PEt 3)N 3 (respectively denoted as AFCN, AFSCN and AFN 3), were prepared and characterized. The crystal structure was solved for Au(PEt 3)SCN highlighting the classical linear geometry of the 2-coordinate gold(I) center. The solution behaviour of the compounds was then comparatively analysed through 31 PNMR providing evidence for an acceptable stability under physiological-like conditions. Afterward, the reaction of these gold compounds with bovine serum albumin (BSA) and consequent adduct formation was investigated by 31 PNMR. For all the studied gold compounds, the [Au(PEt 3)] + moiety was identified as the reactive species in metal/protein adducts formation. The cytotoxic effects of the complexes were subsequently

	measured in comparison to AF against a representative colorectal cancer cell line and found to be still relevant and roughly similar in the three cases though far weaker than those of AF. These results show that the nature of the anionic ligand can modulate importantly the pharmacological action of the gold-triethylphosphine moiety, affecting the cytotoxic potency. These aspects may be further explored to improve the pharmacological profiles of this family of metal complexes.

Structural and solution chemistry, antiproliferative effects, and serum albumin binding of three pseudohalide derivatives of Auranofin

Damino Cirri,[a],* Maria Giulia Fabbrini,[a] Lara Massai,[a] Serena Pillozzi,[b] Annalisa Guerri,[a] Alessio Menconi,[b] Luigi Messori,[a,*] Tiziano Marzo,[c,#] and Alessandro Pratesi[a,#]

[a] Dr. D. Cirri, Dr. M.G. Fabbrini, Dr. L. Massai, Dr. A. Guerri, Prof. Luigi Messori, Dr. Alessandro Pratesi, Department of Chemistry, University of Florence, Via della Lastruccia 3, 50019 Sesto Fiorentino (Italy). E-mail: damiano.cirri@unifi.it; luigi.messori@unifi.it

[b] Dr. S. Pillozzi, Dr. Alessio Menconi, Department of Experimental and Clinical Medicine, University of Florence, Viale GB Morgagni 50, 50134 Firenze (Italy).

[c] Dr. T. Marzo, Department of Pharmacy, University of Pisa, Via Bonanno Pisano 6, 56126, Pisa (Italy).

 # These two authors equally contributed

Abstract. Three pseudohalide analogues of the established gold drug Auranofin (AF hereafter), of general formula $Au(PEt_3)X$, i.e. $Au(PEt_3)CN$, $Au(PEt_3)SCN$ and $Au(PEt_3)N_3$ (respectively denoted as AFCN, AFSCN and AFN_3), were prepared and characterized. The crystal structure was solved for $Au(PEt_3)SCN$ highlighting the classical linear geometry of the 2-coordinate gold(I) center. The solution behaviour of the compounds was then comparatively analysed through ^{31}PNMR providing evidence for an acceptable stability under physiological-like conditions. Afterward, the reaction of these gold compounds with bovine serum albumin (BSA) and consequent adduct formation was investigated by ^{31}PNMR. For all the studied gold compounds, the $[Au(PEt_3)]^+$ moiety was identified as the reactive species in metal/protein adducts formation. The cytotoxic effects of the complexes were subsequently measured in comparison to AF against a representative colorectal cancer cell line and found to be still relevant and roughly similar in the three cases though far weaker than those of AF. These results show that the nature of the anionic ligand can modulate importantly the pharmacological action of the gold-triethylphosphine moiety, affecting the cytotoxic potency. These aspects may be further explored to improve the pharmacological profiles of this family of metal complexes.

Keywords: Metal Based Drugs • NMR • Cancer • Protein Metalation • BSA.

Introduction

The huge costs of new drug development represent a discouraging factor for the obtainment of new anticancer molecules. For this reason, in recent years, chemists working in the field of drug discovery have focused their interest towards drug repurposing strategies (Pushpakom et al. 2019). Indeed, the drug repositioning approach i.e. the use of an already approved drug for different indications, can be a straightforward and convenient way for discovering new active molecules. This is made possible because the investigated molecules have already passed clinical trials and may thus be considered as "safe" in this contex. In this frame, a very promising metal-based compound that has attracted increasing attention as a potential anticancer chemotherapy agent is AF (Ridaura®), an orally administered gold-based drug in clinical use for the treatment of a few severe forms of rheumatoid arthritis since 1988 (Roder and Thomson 2015; May et al. 2018). In recent years, several papers have been published highlighting the antineoplastic activity of AF against several cancer models with an acceptable systemic toxicity (Landini et al. 2017; Hou et al. 2018). Based on its promising features, AF has entered clinical trials in the U.S. against various liquid and solid tumours (Marzo et al. 2019; Database of privately and publicly funded clinical studies conducted around the world.).

One of the most important mechanisms for AF anticancer activity relies in the impairment of key enzymes responsible for the maintenance of the redox homeostasis of cells. Among them, thioredoxin reductase bears a selenocysteine moiety in the active redox site that is reputed as the main site for gold coordination eventually causing potent protein inhibition (Fabbrini et al. 2018). However, it is nowadays widely ascertained that also other proteins may react with AF modulating its bioavailability and biodistribution. Serum albumin is the most abundant plasma protein and it is able to react with AF even upon short incubation times (Clinical Pharmacokinetics II 1986; Massai et al. 2019). As a consequence, human serum albumin (HSA) turns out to be the major carrier for AF in the blood (Talib et al. 2006). Indeed, this protein is the most abundant protein in plasma, with a concentration of approximately 0.6 mM (Fanali et al. 2012). Its main physiological functions include maintenance of the pH and osmotic pressure of plasma, and transport of a variety of endogenous and exogenous substances, including metal ions (Marcon et al. 2003; Singh et al. 2018). Serum albumin consists of a single polypeptide chain of 585 amino acids including 35 cysteine residues, all of which except Cys34 are normally involved in disulfide bonds. Indeed, the unique cysteine residue Cys34 is present either as a free thiol (~40%), or bound to an endogenous thiol such as cysteine, homocysteine or glutathione (Lee and Wu 2015). The peculiar topology of the Cys34 site accounts for its unambiguous involvement in Au(I) (i.e. AF) and Pt(II) (i.e. cisplatin) complexes formation (Sokolowska et al. 2009).

A convenient way to extend the drug repurposing approaches for new drug discovery is to slightly modify the structure of already known active molecules, leaving unaltered the interaction abilities with serum proteins that are typical of the Au(I) complexes (Pratesi et al. 2018). Starting from these premises our research group had previously screened two derivatives of AF in which the thiosugar moiety had been replaced with chloride and iodide respectively obtaining some interesting results (Marzo et al. 2017; Marzo et al. 2019). In this frame, we have decided to further expand the panel of AF derivatives. We also realised that satisfactory biological reports focused on the binding to serum albumin of AF pseudohalide analogues were missing in the literature. For these reasons, we decided to synthesize and fully characterise three compounds (Fig.1), with a common chemical structure based on $Au(PEt_3)X$, where X is a pseudohalide group (-CN; -SCN or $-N_3$). The study is aimed to elucidate the stability of these gold compounds in physiological like buffers, to assess their solution behaviour in comparison with AF when incubated with a thiol-bearing protein such bovine serum albumin (BSA) and to determine their antiproliferative actions *in vitro*.

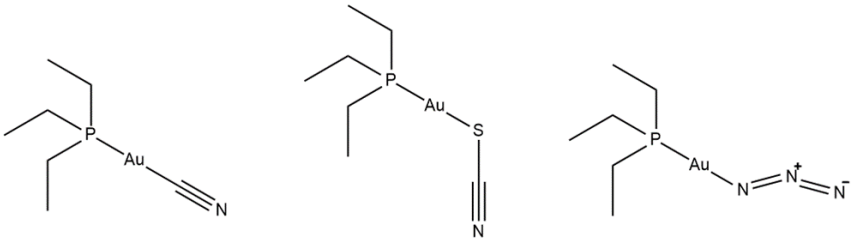

Fig. 1. Chemical structure of the investigated compounds.

Materials and Methods

2.1. General

All materials were purchased from Sigma-Aldrich, Merck or Honeywell and were used without further purification. LogP was determined through shake-flask method. The quantitation of compounds in the pre-saturated water or octanol phase was carried out by ICP-AES analysis following a procedure already established in our lab (Cirri et al. 2017).

2.2. Synthesis and Characterization

AFCN was synthesized according to the procedure reported in scheme 1A, using a ligand scrambling reaction. The desired product was obtained by an extraction process from water/low polarity solvent (such as chloroform) mixture. AFSCN and AFN_3 were prepared as displayed in scheme 1B, through activation of the gold-triethylphosphine moiety with silver nitrate. All the synthesized products were characterized by elemental analysis and ^{31}PNMR.

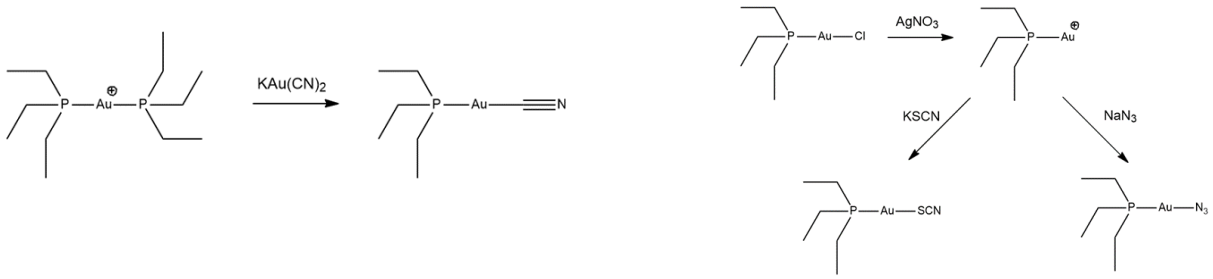

A **B**

Scheme 1. Reaction pathways for the synthesis of AFCN, AFSCN and AFN_3

AFCN

AFCN was synthesized using the scrambling reaction reported in literature (Hormann-Arendt and Shaw III 1990). In a flask were added 5 mL of chloroform, 2 mL of MilliQ water, 31.08 mg (0.066 mmol; 1 eq.) of $[Au(PEt_3)_2]Cl$ and 21.00 mg (0.073 mmol; 1.11 eq.) of $K[Au(CN)_2]$ (both compounds were previously synthesized as described in (Marzo et al. 2018). The biphasic mixture was stirred at room temperature for 4h, then the organic phase was recovered using a separation funnel and dried under vacuum. The crude product was dissolved in 0.5 mL of $CHCl_3$ and precipitated as white small crystals immediately after adding 5 mL of Et_2O (26.8 mg; 59.3% yield). Characterization was carried out by ^{1}H, ^{13}C and ^{31}PNMR. The purity of product was assessed by CHN analysis: [Calculated C: 24.65 % H: 4.43 % N: 4.11 %; Experimental C: 24.72 % H: 4.54 % N: 3.89 %].
LogP: 0.8
^{1}HNMR ($CDCl_3$; 400.13 MHz): 1.84 (dq; J_{HH} = 7.68 Hz; J_{PH} = 9.86 Hz; 6H); 1.21 (dt; J_{HH} = 7.65 Hz; J_{PH} = 18.59 Hz; 9H)
^{31}PNMR ($CDCl_3$; 161.98 MHz): 36.05
^{13}CNMR ($CDCl_3$; 100.61 MHz): 159.39; 18.16 (d; J_{CP} = 34.58 Hz); 9.52

AFSCN

AFSCN was synthesized modifying an existing experimental protocol (El-Etri and Scovell 1990). In a flask were added 39.45 mg of $Au(PEt_3)Cl$ (0.112 mmol; 1 eq.), 5 mL of EtOH and 19.12 mg of $AgNO_3$ (0.112 mmol: 1 eq.). The suspension was stirred for 1h at 25° C and filtered to remove the AgCl formed. The liquid phase was moved in a clean flask and 10.49 mg (0.108 mmol; 0.96 eq.) of KSCN were added. The suspension was stirred for 1.5 h and dried under vacuum. The crude product was dissolved in 5 mL of dichloromethane and 5 mL of H_2O. The biphasic mixture was moved in a separation funnel and the organic phase was recovered. The aqueous phase was re-extracted with 5 mL of dichloromethane and the recovered organic ones were diluted with 7 mL of chloroform and washed with 5 mL of MilliQ water. The organic phase was then dried with $MgSO_4$ and evaporated under vacuum. The crude product was solubilized in 0.5 mL of dichloromethane and 5 mL of diethyl ether were added and the flask was kept at -20°C for 72 h. After this time some white crystals were formed at the bottom of the flask. Next, 10 mL of hexane were added and the

flask was kept at -20°C for further 24 h. 25.25 mg of white crystals of the desired product were collected (yield 60.1%). Characterization was performed by ^{1}H, ^{13}C, ^{31}PNMR and X-Ray crystallography. The purity of product was assessed by CHN analysis: [Calculated C: 22.53 % H: 4.05 % N: 3.75 %; Experimental C: 22.52 % H: 4.25 % N: 3.50 %].
LogP: 0.6
^{1}HNMR ($CDCl_3$; 400.13 MHz): 1.89 (dq; J_{HH} = 7.66 Hz; J_{PH} = 10.06 Hz; 6H); 1.23 (dt; J_{HH} = 7.64 Hz; J_{PH} = 19.00 Hz; 9H)
^{31}PNMR ($CDCl_3$; 161.98 MHz): 36.63
^{13}CNMR ($CDCl_3$; 100.61 MHz): 18.48 (d; J_{CP} = 35.04 Hz); 9.66

AFN_3

AFN_3 was synthesized modifying the procedure described in literature (El-Etri and Scovell 1990). In a flask were added 53.91 mg (0.154 mmol; 1 eq.) of $Au(PEt_3)Cl$, 4 mL of EtOH and 26.12 mg of $AgNO_3$ (0.154 mmol; 1 eq.). The suspension was stirred for 1h at r.t. and AgCl filter-off. The liquid phase was moved in a flask and 10.01 mg (0.154 mmol; 1 eq.) of NaN_3 were added. The suspension was stirred for 2h at r.t, then 10 mL of hexane were added. After 10 minutes of stirring the suspension was filtered once again for the removal of formed $NaNO_3$, then further 10mL of hexane were added. The flask was kept at -20°C for 24 h, after this time, crystals were formed at the bottom of flask. The product was recovered as 30.18 mg of white crystals (yield 54.9%). Characterization was performed by ^{1}H, ^{13}C and ^{31}PNMR. The purity of product was assessed by CHN analysis: [Calculated C: 20.18 % H: 4.23 % N: 11.77 %; Experimental C: 19.80 % H: 3.86 % N: 10.68 %].
LogP: 0.6
^{1}HNMR ($CDCl_3$; 400.13 MHz): 1.82 (dq; J_{HH} = 7.66 Hz; J_{PH} = 10.20 Hz; 6H); 1.19 (dt; J_{HH} = 7.63 Hz; J_{PH} = 18.75 Hz; 9H)
^{31}PNMR ($CDCl_3$; 161.98 MHz): 28.78
^{13}CNMR ($CDCl_3$; 100.61 MHz): 19.30 (d; J_{CP} = 37.25 Hz); 10

2.3. NMR studies

All NMR spectra were recorded on a Bruker Avance III spectrometer equipped with a Bruker Ultrashield 400 Plus superconducting magnet. Measurements took place at 400.13 MHz (^{1}H) 161.98 MHz (^{31}P) and 100.61 MHz (^{13}C).

2.4. X-ray analysis

X-ray diffraction data were collected on an Oxford Diffraction Xcalibur3 instrument with Mo Kα radiation (λ = 0.71073 Å) and at a temperature of 100 K. The software suite CrysAlisPro (CrysAlisPro 1.171.38.41r 2015) was then used for the data collection and data reduction. Absorption correction was applied with the program SCALE3 ABSPACK, also integrated in the CrysAlisPro package.
The structure was solved by using the direct methods implemented in Sir97 program (Altomare et al. 1999) and refined by full-matrix least-squares techniques using SHELXL-2013 (Thorn et al. 2012) with anisotropic displacement parameters for all non-hydrogen atoms. The hydrogen atoms in AFSCN were introduced in calculated positions and refined considering a riding model with isotropic thermal parameters. After the final refinement, due to the presence of heavy atoms in the molecule and to a not high redundancy, some residual electron density can still be found in the map. Geometrical calculations were performed by using the program PARST (Nardelli 1995) and molecular plots were produced with ORTEP3 (Farrugia 1997), both implemented in the Crystal Structure crystallographic software package WINGX (Farrugia 2012).
All the crystal data and refinement parameters shown in Table S1 and Table S2. CCDC 1910813 contains the supplementary crystallographic data for this paper. These data can be obtained free of charge from the Cambridge Crystallographic Data Centre via http://www.ccdc.cam.ac.uk/Community/Requestastructure.

2.5. Cell cultures

HCT116 cells were cultured in RPMI-1640 medium with 10% Fetal Bovine Serum (FBS), at 37 °C in humidified atmosphere and 5% CO_2 in air. Drugs were solubilised in DMSO prior to be used for biological experiments at 30 mM concentration. The subsequent solutions resulted by dilutions in accurate volumes of RPMI medium.

2.6. Cell viability assay

Cell lines were plated in 96-well plates at a cell density of $1*10^4$ per well in RPMI complete medium. Cells were incubated for 24 h at 37 °C, before the compounds were added at 0, 180 nM, 250 nM, 500 nM, 1 μM. Then, cells were further incubated for 24 h at 37 °C. Finally, cells were harvested, and alive cells were counted using a haemocytometer through the Trypan Blue exclusion assay. The tests were set in triplicate and values were obtained averaging them.

Results and Discussion

3.1. Synthesis and Characterisation

The three compounds were synthesised according to the procedure described in the experimental section and obtained in high purity and high yield. The quality of the obtained products was characterised through a variety of analytical determinations and physicochemical measurements as reported in the experimental section.

3.2. Crystal structure of AFSCN

In the case of AFSCN, crystals suitable for X-ray diffraction analysis were obtained and the corresponding crystal structure solved. The asymmetric unit (a.u.) contains two molecules of the gold complex. The metal ion in both molecules is linearly coordinated being the angles 177.61(11) and 172.78(14)° respectively for P(1)-Au(1)-S(1) and P(2)-Au(2)-S(2). Bond length and angles are in the range of similar compounds retrieved in the CSD. (v. 5.39 November 2017 + 3 updates) (Allen 2002).
The intermetallic distance Au(1)-Au(2) between the two molecules is 3.4579(7) Å, which is frequently found in this kind of linear complexes (CSD).

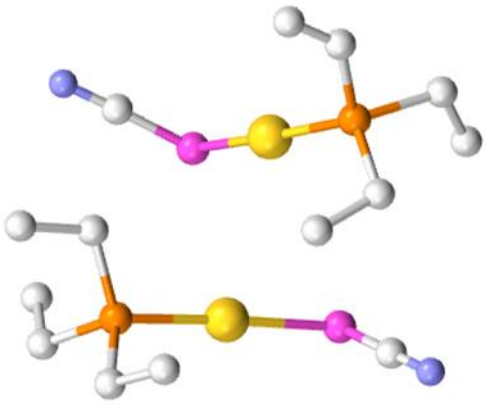

Fig. 2. The crystal structure of AFSCN.

3.3. Solution behaviour

The solution stability of the three gold compounds was assessed through ^{31}PNMR. Spectra were acquired both in DMSO-d_6 and in a mixture 9:1 of buffer phosphate (50mM pH 7.4) and DMSO-d_6 at 0, 24 h, 48 h and 72 h.
For both AFCN and AFSCN it is possible to observe a ligand displacement process leading to the formation of the $[Au(PEt_3)]^+$ cation.
Moreover, when solubilized in pure dimethyl sulfoxide, AFSCN allows the formation of a new species detected at 33.9 ppm in ^{31}P-NMR. This species was identified through ESI-MS investigation as a binuclear cation with raw formula of $[Au_2(PEt_3)_2SCN]^+$ (see supporting information, Fig.S14). Conversely, no spectral changes were observed in the same conditions for AFN_3 (see figure S15, S16).

3.4. Interactions with BSA monitored by ^{31}PNMR measurements

The interactions of $Au(PEt_3)CN$, $Au(PEt_3)SCN$ and $Au(PEt_3)N_3$ with BSA were previously analysed by ESI-MS in a methodological study (Pratesi et al. 2018). This study and its results have now been complemented by independent ^{31}PNMR measurements.
^{31}PNMR experiments were carried out on samples where 35 mg of BSA were mixed with one equivalent of $Au(PEt_3)X$ (X = CN; SCN; N_3) and solubilised under controlled temperature through sonication in 0.5 mL of D_2O. The spectra were acquired at t_0 and after 24 h of incubation at 37 °C, pH was checked at the end of each measurement and no changes were found. As reported in figure 5, AFCN (36.5 ppm) reacted immediately with BSA forming an $AlbSAuPEt_3$ derivative. The latter species is characterized by a ^{31}PNMR signal located at 42.0 ppm (Isab, Shaw III et al. 1988; Coffer et al. 1987; Isab, Hormann et al. 1988); during this reaction a conspicuous amount of the $[Au(PEt_3)_2]^+$ cation (47.0 ppm) was formed that is usually found in tiny amounts as a side product (Marzo et al. 2017; Coffer et al. 1986). The formation of $[Au(PEt_3)_2]^+$ can be easily explained by the scrambling reaction of AFCN described in literature, accompanied by the formation of the $[Au(CN)_2]^-$ anion (Marzo et al. 2017). Noteworthy, the discrepancy (3 ppm) in the chemical shifts of the detected species in comparison with those reported in literature (Isab, Shaw III et al. 1988; Coffer et al. 1987; Isab, Hormann et al. 1988; Coffer et al. 1986) is the consequence of a calibration in the NMR experiments on $OP(OCH_3)_3$ instead on H_3PO_4. The equilibrium constant for the reaction that these systems undergo, was shown to be dependent upon the solvent, increasing with the polarity and/or polarizability of the solvent itself (Marzo et al. 2018).
After 24 h of incubation the presence of the $AlbSAuPEt_3$ adduct was still detected. Furthermore, a complete disappearing of both free AFCN and the Au-diphosphine cationic scrambling product was observed, as well as the concomitant formation of $POEt_3$ specie. These data let us to confirm the mechanism proposed for the binding of AFCN to albumin (Isab, Hormann et al. 1988).
On the whole, the Au/BSA interaction process can be summarised as below:
1) AFCN releases the CN^- anion when the bound with thiolic residue in Cys34 takes place.
2) The $AlbSAuPEt_3$ adduct releases a phosphine molecule triggered by the reaction with the cyanide anion generated in the first step, leading to the formation of a new AlbSAuCN adduct.
3) The released phosphine moiety was finally oxidized to the corresponding triethylphosphine oxide, likely provoking the subsequent reduction of some disulphide bridges present in BSA.

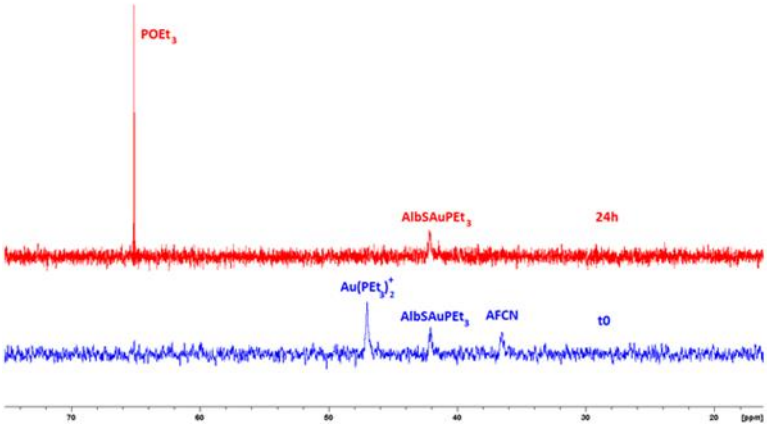

Fig. 3. NMR Spectrum of AFCN 1 mM + BSA 1 mM in D2O at t_0 (blue) and after 24h of incubation at 37°C (red).

Despite the similarity of their chemical structures, the reactivity of AFSCN turned out to be different respect to AFCN. Indeed, upon incubating AFSCN in the same condition, a quantitative formation of AlbSAuPEt$_3$ adduct was observed at t_0 (Fig.5). Moreover, after 24 h of incubation a more complex speciation was detected. Indeed, it was possible to observe the formation of a small amount of $[Au(PEt_3)_2]^+$ cation, a backformation of AFSCN (broad signal at 38.1 ppm) and the generation of the dinuclear cation $[Au_2(PEt_3)_2SCN]^+$ at 32.9 ppm.

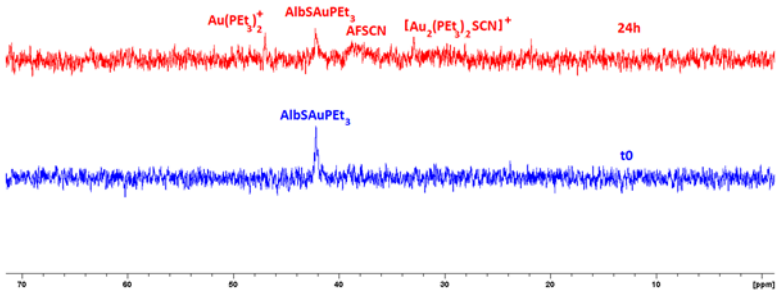

Fig. 4. NMR Spectrum of AFSCN 1 mM + BSA 1 mM in D_2O at t_0 (blue) and after 24h of incubation at 37°C (red).

AFN_3 was also analysed following the same experimental protocol. As reported in figure 5, and similarly to AFSCN, AFN_3 turned out to give a rapid and quantitative formation of AlbSAuPEt$_3$ adduct at t_0 and after 24 h of incubation no changes were detected in the spectrum. This lack of further reactivity during the incubation was probably due to the lower affinity of the released azido group towards Au(I) compared to the cyanide or thiocyanate anions. In fact, the released azido residue seemed to be unable to further interact with the formed AlbSAuPEt$_3$ adduct.

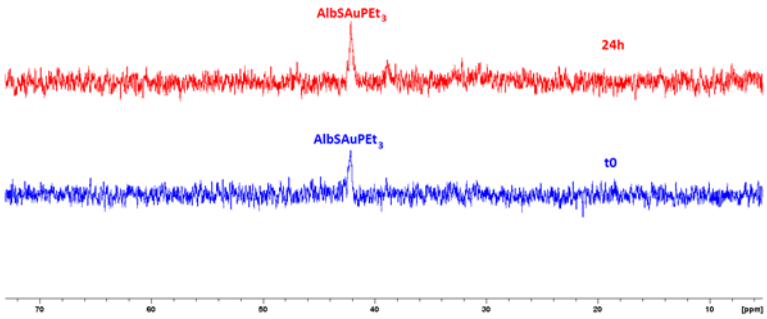

Fig. 5. NMR Spectrum of AFN_3 1 mM + BSA 1 mM in D_2O at t0 (blue) and after 24h of incubation at 37°C (red).

3.5. Cytotoxicity assays

The cytotoxic effects of the three compounds were assessed *in vitro* toward a representative CRC cell line, HCT116 (Fig 6 and supporting material). The effects were tested by the trypan blue exclusion assay, after 24 h of incubation. First of all, single dose experiments were carried out on the ground of the IC_{50} value of AF, which has been recently published by our group (Marzo et al. 2017).

We observed that the three compounds did not exert a remarkable activity at 180 nM (being this the value of AF IC_{50} HCT116 cells in the same experimental condition). Only AFCN shows a slightly cytotoxic action (Fig. 6A).

Thus, we decided to expose HCT116 cells to greater concentrations of the three study compounds: 250 nM, 500 nM up to 1 μM (~5 times higher than IC_{50} of AF). However, AFCN, AFSCN and AFN_3 do not show relevant cytotoxic proprieties even at these concentrations (Fig. 6B).

In a third experiment we exposed HCT116 cells to a 10 μM concentration of the three study compounds; in this latter case we observe nearly complete inhibition of cell growth. These results suggest that the IC_{50} values of the three compounds are almost comparable in the three cases and roughly fall in the concentration interval 3-8 μM. Thus, AFCN, AFSCN and AFN_3 appear to be far less active than AF but still remarkably cytotoxic with IC50 values <10 μM.

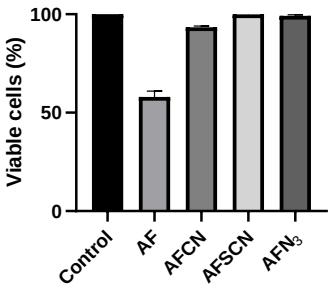

A

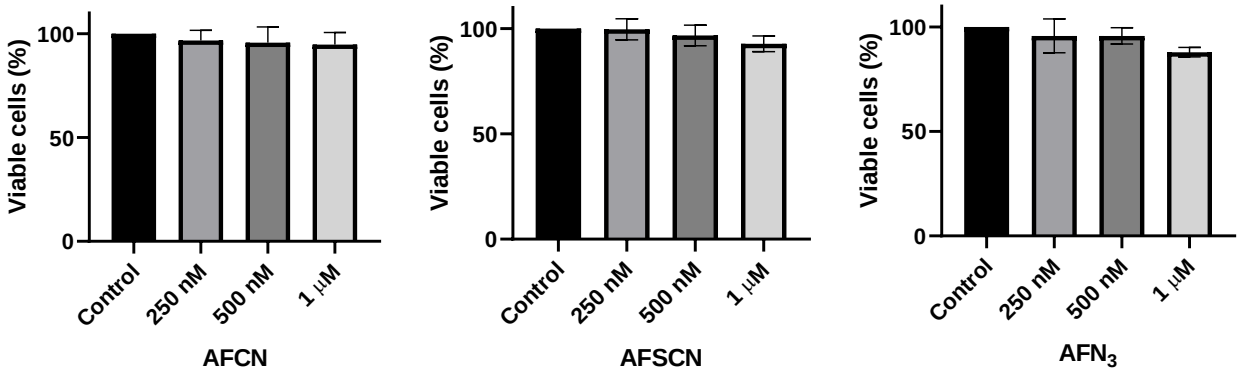

B

Fig. 6. Evaluation of cytotoxic activity of AFCN, AFSCN and AFN_3 in HCT116 cells. Cell viability was investigated after 24 h of treatment by the trypan blue exclusion assay. The column graphs represent the effect of the compounds in term of percentage of viable HCT116 cells. Viable cells were counted in triplicate, using a haemocytometer. A) AFCN, AFSCN and AFN3 were tested at a representative concentration i.e. IC_{50} of AF, 180 nM. B) The compounds, respectively AFCN, AFSCN and AFN_3, were tested at 250 nM, 500 nM and 1 μM.

Conclusions

Here, we have reported on the synthesis and the chemical characterization of three AF derivatives where the thiosugar ligand is replaced by a pseudohalide ligand, i.e. cyanide, thiocyanate and azide, respectively. For one of them i.e. AFSCN, the crystal structure has been solved revealing a classical linear coordination at the gold(I) center in line with expectations. The solution behaviour of these gold compounds was analysed comparatively by ^{31}PNMR. This analytical technique permits to monitor the stability and the chemical transformations. Moreover, ^{31}PNMR was also exploited to analyse the molecular interactions of these gold compounds with bovine serum albumin. Lastly, these compounds were studied for their antiproliferative properties toward the HCT116 cancer cell line. Results revealed quite different pharmacological profiles: notably, the replacement of the thiosugar with a pseudohalide did not lead to loss of the biological activity confirming that the thiosugar moiety is not essential for pharmacological activity, in line with previous observations on the halide derivatives (Marzo et al. 2017). Rather, we observed some remarkable attenuation of the cytotoxic properties; these results clearly imply that the nature of the anionic ligand can modulate heavily the pharmacological

activity of $Au(PEt_3)X$ metal complexes, suggesting that the biological profile could be improved with simple chemical modifications of the molecule. Indeed, the overall activity of the metal complex is significantly linked to the nature of X^- group, that is reasonable to assume to be acting as the leaving group. The affinity of the ligands toward the gold centre strongly affects the existing equilibria with an important impact into the pharmacological effects that are exerted by the active cationic species $[Au(PEt_3)]^+$. Additionally, differences in the antiproliferative actions may be broadly correlated with differences in the reactivity with target proteins. To this end the study of the interactions with BSA here reported may represent a simple and instructive model.

Acknowledgements

D. C. gratefully acknowledge Associazione Italiana per la Ricerca sul Cancro for the financial support (AIRC 1-year Fellowship for Italy – Project Code: 22294). L. M. gratefully acknowledges AIRC (Associazione Italiana per la Ricerca sul Cancro) and ECRF (Ente Cassa di Risparmio di Firenze) for the financial support (AIRC-ECRF19650). CIRCMSB and ente CRF are also acknowledged. T.M. thanks University of Pisa (Rating Ateneo 2018/2019) for the financial support.

References

Allen F H (2002) The Cambridge Structural Database: a quarter of a million crystal structures and rising. Acta Cryst. B58:380-388.

Altomare A, Burla M C, Camalli M, Cascarano G L, Giacovazzo C, Guagliardi A, Moliterni A G G, Polidori G, Spagna R (1999) SIR97: a new tool for crystal structure determination and refinement. J. Appl. Cryst. 32:115-119.

Cirri D, Pillozzi S, Gabbiani C, Tricomi J, Bartoli G, Stefanini M, Michelucci E, Arcangeli A, Messori L, Marzo T (2017) PtI_2(DACH), the iodido analogue of oxaliplatin as a candidate for colorectal cancer treatment: chemical and biological features. Dalton Trans. 46:3311-3317.

Clinical Pharmacokinetics II (1986) 133-143.

Coffer M T, Shaw III C F, Eidsness M K, Watkins II J W, Elder R C (1986) Reactions of auranofin and chloro(triethylphosphine)gold with bovine serum albumin. Inorg. Chem. 25:333-339.

Coffer M T, Shaw III C F, Hormann A L, Mirabelli C K, Crooke S T (1987) Thiol competition for Et_3PAuS-albumin: a nonenzymatic mechanism for Et_3PO formation. J. Inorg Biochem. 30:177-187.

CrysAlisPro 1.171.38.41r, (2015) Rigaku Oxford Diffraction.

Database of privately and publicly funded clinical studies conducted around the world; https://clinicaltrials.gov

El-Etri M M, Scovell W M (1990) Synthesis and Spectroscopic Characterization of (Triethylphosphine)gold(I) Complexes $AuX(PEt_3)$ (X = Cl, Br, CN, SCN), $[AuL(PEt_3)^+]$ (L = SMe_2, $SC(NH_2)_2$, H_2O), and $(\mu$-S)$[Au(PEt_3)]_2$. Inorg Chem. 29:480-484.

Fabbrini M G, Cirri D, Pratesi A, Ciofi L, Marzo T, Guerri A, Nistri S, Dell'Accio A, Gamberi T, Severi M, Bencini A, Messori L (2018) Chem. Med. Chem. 13:1-8.

Fanali G, di Masi A, Trezza V, Marino M, Fasano M, Ascenzi P (2012) Human serum albumin: from bench to bedside. Molecular Aspects of Medicine 33:209-290.

Farrugia L J (1997) ORTEP-3 for Windows - a version of ORTEP-III with a Graphical User Interface (GUI). J. Appl. Cryst. 30:565.

Farrugia L J (2012) WinGX and ORTEP for Windows: an update. J. Appl. Cryst. 45:849-854.

Hormann-Arendt A L, Shaw III C F (1990) Ligand-scrambling reactions of cyano(trialkyl/triarylphosphine)gold(I) complexes: examination of factors influencing the equilibrium constant. Inorg Chem. 29:4683-4687.

Hou G X, Liu P P, Zhang S, Yang M, Liao J, Yang J, Hu Y, Jiang W Q, Wen S, Huang P (2018) Elimination of stem-like cancer cell side-population by auranofin through modulation of ROS and glycolysis Cell Death and Disease 9:89-103.

Isab A A, Hormann A L, Coffer M T, Shaw III C F (1988) Reversibly and Irreversibly Formed Products from the Reactions of Mercaptalbumin (AlbSH) with Et_3PAuCN and of $AlbSAuPEt_3$ with HCN. J. Am. Chem. Soc. 110:3278-3284.

Isab A A, Shaw III C F, Hoeschele J D, Locke J (1988) Reactions of trimethylphosphine analogs of auranofin with bovine serum albumin. Inorg. Chem. 27:3588-3592.

Landini I, Lapucci A, Pratesi A, Massai L, Napoli C, Perrone G, Pinzani P, Messori L, Mini E, Nobili S (2017) Selection and characterization of a human ovarian cancer cell line resistant to auranofin. Oncotarget 8:96062-96078.

Lee P, Wu X (2015) Review: modifications of human serum albumin and their binding effect. Curr. Pharm. Des. 21:1862-1865.

Marcon G, Messori L, Orioli P, Cinellu M A, Minghetti G (2003) Reactions of gold(III) complexes with serum albumin. Eur. J. Biochem. 270:4655-4661.

Marzo T, Cirri D, Gabbiani C, Gamberi T, Magherini F, Pratesi A, Guerri A, Biver T, Binacchi F, Stefanini M, Arcangeli A, Messori L (2017) Auranofin, Et_3PAuCl, and Et_3PAuI Are Highly Cytotoxic on Colorectal Cancer Cells: A Chemical and Biological Study ACS Med. Chem. Lett. 8:997-1001.

Marzo T, Cirri D, Pollini S, Prato M, Fallani S, Cassetta M I, Novelli A, Rossolini G M, Messori L (2018) Auranofin and its Analogues Show Potent Antimicrobial Activity against Multidrug-Resistant Pathogens: Structure–Activity Relationships. ChemMedChem. 13:2448–2454.

Marzo T, Massai L, Pratesi A, Stefanini M, Cirri D, Magherini F, Becatti M, Landini I, Nobili S, Mini E, Crociani O, Arcangeli A, Pillozzi S, Gamberi T, Messori L (2019)

Replacement of the Thiosugar of Auranofin with Iodide Enhances the Anticancer Potency in a Mouse Model of Ovarian Cancer. ACS Med. Chem. Lett. 10:656-660.

Massai L, Pratesi A, Gailer J, Marzo T, Messori L (2019) The cisplatin/serum albumin system: A reappraisal. Inorganica Chimica Acta 495:118983-118989.

May H C, Yu J J, Guentzel M N, Chambers J P, Cap A P, Arulanandam B P (2018) Repurposing Auranofin, Ebselen, and PX-12 as Antimicrobial Agents Targeting the Thioredoxin System. Front. Microbiol. 9:336-345.

Nardelli M (1995) PARST95 - an update to PARST: a system of Fortran routines for calculating molecular structure parameters from the results of crystal structure analyses. J. Appl. Cryst. 28:659.

Pratesi A, Cirri D, Ciofi L, Messori L (2018) Reactions of Auranofin and Its Pseudohalide Derivatives with Serum Albumin Investigated through ESI-Q-TOF MS. Inorg. Chem. 57:10507-10510.

Pushpakom S, Iorio F, Eyers P A, Escott K J, Hopper S, Wells A, Doig A, Guilliams T, Latimer J, McNamee C, Norris A, Sanseau P, Cavalla D, Pirmohamed M (2019) Drug repurposing: progress, challenges and recommendations. Nature Reviews Drug Discovery 18:41-58.

Roder C, Thomson M J (2015) Auranofin: repurposing an old drug for a golden new age. Drugs R. D. 15:13-20.

Singh N, Pagariya D, Jain S, Naik S, Kishore N (2018) Interaction of copper (II) complexes by bovine serum albumin: spectroscopic and calorimetric insights. Journal of Biomolecular Structure and Dynamics 9:2449-2462.

Sokołowska M, Wszelaka-Rylik M, Poznański J, Bal W (2009) Spectroscopic and thermodynamic determination of three distinct binding sites for Co(II) ions in human serum albumin. J. Inorg. Biochem. 103:1005-1013.

Talib J, Beck J L, Ralph S F (2006) A mass spectrometric investigation of the binding of gold antiarthritic agents and the metabolite $[Au(CN)_2]^-$ to human serum albumin. J. Biol. Inorg. Chem. 11:559-570.

Thorn A, Dittrich B, Sheldrick G M (2012) Enhanced rigid-bond restraints. Acta Cryst. A68:448-451.

checkCIF/PLATON report

Structure factors have been supplied for datablock(s) AFSCN

THIS REPORT IS FOR GUIDANCE ONLY. IF USED AS PART OF A REVIEW PROCEDURE FOR PUBLICATION, IT SHOULD NOT REPLACE THE EXPERTISE OF AN EXPERIENCED CRYSTALLOGRAPHIC REFEREE.

No syntax errors found. CIF dictionary Interpreting this report

Datablock: AFSCN

```
Bond precision:  C-C = 0.0247 A          Wavelength=0.71073

Cell:          a=7.3651(7)       b=12.0894(12)    c=13.4821(12)
               alpha=74.491(8)   beta=83.768(8)   gamma=78.215(8)
Temperature:   100 K
```

	Calculated	Reported
Volume	1130.50(19)	1130.50(19)
Space group	P -1	P -1
Hall group	-P 1	-P 1
Moiety formula	C7 H15 Au N P S	?
Sum formula	C7 H15 Au N P S	C14 H30 Au2 N2 P2 S2
Mr	373.20	746.39
Dx,g cm-3	2.193	2.193
Z	4	2
Mu (mm-1)	13.287	13.287
F000	696.0	696.0
F000’	689.70	
h,k,lmax	10,17,19	10,17,19
Nref	7180	6287
Tmin,Tmax	0.534,0.671	0.241,1.000
Tmin’	0.069	

```
Correction method= # Reported T Limits: Tmin=0.241 Tmax=1.000
AbsCorr = MULTI-SCAN

Data completeness= 0.876          Theta(max)= 30.911

R(reflections)= 0.0511( 3953)     wR2(reflections)= 0.1372( 6287)

S = 1.063                 Npar= 199
```

The following ALERTS were generated. Each ALERT has the format
test-name_ALERT_alert-type_alert-level.
Click on the hyperlinks for more details of the test.

Alert level A

PLAT973_ALERT_2_A Check Calcd Positive Resid. Density on Au1 2.70 eA-3
PLAT973_ALERT_2_A Check Calcd Positive Resid. Density on Au2 2.12 eA-3

Alert level B

PLAT342_ALERT_3_B Low Bond Precision on C-C Bonds ..... 0.02467 Ang.
PLAT919_ALERT_3_B Reflection # Likely Affected by the Beamstop ... 1 Check

Alert level C

PLAT220_ALERT_2_C Non-Solvent Resd 2 C Ueq(max)/Ueq(min) Range 4.9 Ratio
PLAT222_ALERT_3_C Non-Solv. Resd 2 H Uiso(max)/Uiso(min) Range 6.0 Ratio
PLAT241_ALERT_2_C High 'MainMol' Ueq as Compared to Neighbors of S2 Check
PLAT241_ALERT_2_C High 'MainMol' Ueq as Compared to Neighbors of C3 Check
PLAT242_ALERT_2_C Low 'MainMol' Ueq as Compared to Neighbors of Au2 Check
PLAT242_ALERT_2_C Low 'MainMol' Ueq as Compared to Neighbors of P2 Check
PLAT242_ALERT_2_C Low 'MainMol' Ueq as Compared to Neighbors of C2 Check
PLAT242_ALERT_2_C Low 'MainMol' Ueq as Compared to Neighbors of C5 Check
PLAT260_ALERT_2_C Large Average Ueq of Residue Including Au2 0.119 Check
PLAT360_ALERT_2_C Short C(sp3)-C(sp3) Bond C5 - C11 . 1.42 Ang.
PLAT413_ALERT_2_C Short Inter XH3 .. XHn H11B ..H11C . 2.02 Ang.
-x,2-y,-z = 2_575 Check
PLAT906_ALERT_3_C Large K Value in the Analysis of Variance ..... 3.303 Check
PLAT918_ALERT_3_C Reflection(s) with I(obs) much Smaller I(calc) . 1 Check
PLAT934_ALERT_3_C Number of (Iobs-Icalc)/SigmaW > 10 Outliers .... 1 Check
PLAT939_ALERT_3_C Large Value of Not (SHELXL) Weight Optimized S . 12.50 Check
PLAT971_ALERT_2_C Check Calcd Resid. Dens. 2.00A From S2 1.79 eA-3
PLAT971_ALERT_2_C Check Calcd Resid. Dens. 1.05A From S1 1.72 eA-3
PLAT971_ALERT_2_C Check Calcd Resid. Dens. 0.90A From Au2 1.67 eA-3
PLAT972_ALERT_2_C Check Calcd Resid. Dens. 0.82A From Au2 -1.70 eA-3
PLAT978_ALERT_2_C Number C-C Bonds with Positive Residual Density. 0 Info

Alert level G

PLAT002_ALERT_2_G Number of Distance or Angle Restraints on AtSite 6 Note
PLAT045_ALERT_1_G Calculated and Reported Z Differ by a Factor ... 2.00 Check
PLAT154_ALERT_1_G The s.u.'s on the Cell Angles are Equal ..(Note) 0.008 Degree
PLAT172_ALERT_4_G The CIF-Embedded .res File Contains DFIX Records 1 Report
PLAT343_ALERT_2_G Unusual sp3 Angle Range in Main Residue for C5 Check
PLAT432_ALERT_2_G Short Inter X...Y Contact C11 ..C11 3.05 Ang.
-x,2-y,-z = 2_575 Check
PLAT860_ALERT_3_G Number of Least-Squares Restraints ..... 3 Note
PLAT912_ALERT_4_G Missing # of FCF Reflections Above STh/L= 0.600 893 Note

---

2 **ALERT level A** = Most likely a serious problem - resolve or explain
2 **ALERT level B** = A potentially serious problem, consider carefully
20 **ALERT level C** = Check. Ensure it is not caused by an omission or oversight
8 **ALERT level G** = General information/check it is not something unexpected

2 ALERT type 1 CIF construction/syntax error, inconsistent or missing data
20 ALERT type 2 Indicator that the structure model may be wrong or deficient
8 ALERT type 3 Indicator that the structure quality may be low
2 ALERT type 4 Improvement, methodology, query or suggestion
0 ALERT type 5 Informative message, check

It is advisable to attempt to resolve as many as possible of the alerts in all categories. Often the minor alerts point to easily fixed oversights, errors and omissions in your CIF or refinement strategy, so attention to these fine details can be worthwhile. In order to resolve some of the more serious problems it may be necessary to carry out additional measurements or structure refinements. However, the purpose of your study may justify the reported deviations and the more serious of these should normally be commented upon in the discussion or experimental section of a paper or in the "special_details" fields of the CIF. checkCIF was carefully designed to identify outliers and unusual parameters, but every test has its limitations and alerts that are not important in a particular case may appear. Conversely, the absence of alerts does not guarantee there are no aspects of the results needing attention. It is up to the individual to critically assess their own results and, if necessary, seek expert advice.

Publication of your CIF in IUCr journals

A basic structural check has been run on your CIF. These basic checks will be run on all CIFs submitted for publication in IUCr journals (*Acta Crystallographica, Journal of Applied Crystallography, Journal of Synchrotron Radiation*); however, if you intend to submit to *Acta Crystallographica Section C* or *E* or *IUCrData*, you should make sure that full publication checks are run on the final version of your CIF prior to submission.

Publication of your CIF in other journals

Please refer to the *Notes for Authors* of the relevant journal for any special instructions relating to CIF submission.

Validation response form

Please find below a validation response form (VRF) that can be filled in and pasted into your CIF.

```
# start Validation Reply Form
_vrf_PLAT973_AFSCN
;
PROBLEM: Check Calcd Positive Resid. Density on       Au1       2.70 eA-3
RESPONSE: ...
;
_vrf_PLAT220_AFSCN
;
PROBLEM: Non-Solvent  Resd 2  C   Ueq(max)/Ueq(min) Range        4.9 Ratio
RESPONSE: ...
;
_vrf_PLAT222_AFSCN
;
PROBLEM: Non-Solv.  Resd 2  H   Uiso(max)/Uiso(min) Range        6.0 Ratio
RESPONSE: ...
;
_vrf_PLAT241_AFSCN
;
PROBLEM: High   'MainMol' Ueq as Compared to Neighbors of         S2 Check
RESPONSE: ...
;
_vrf_PLAT242_AFSCN
;
PROBLEM: Low    'MainMol' Ueq as Compared to Neighbors of        Au2 Check
RESPONSE: ...
;
_vrf_PLAT260_AFSCN
```

```
;
PROBLEM: Large Average Ueq of Residue Including       Au2      0.119 Check
RESPONSE: ...
;
_vrf_PLAT360_AFSCN
;
PROBLEM: Short  C(sp3)-C(sp3) Bond  C5       - C11      .       1.42 Ang.
RESPONSE: ...
;
_vrf_PLAT413_AFSCN
;
PROBLEM: Short Inter XH3 .. XHn     H11B     ..H11C     .       2.02 Ang.
RESPONSE: ...
;
_vrf_PLAT906_AFSCN
;
PROBLEM: Large K Value in the Analysis of Variance ......      3.303 Check
RESPONSE: ...
;
_vrf_PLAT918_AFSCN
;
PROBLEM: Reflection(s) with I(obs) much Smaller I(calc) .          1 Check
RESPONSE: ...
;
_vrf_PLAT934_AFSCN
;
PROBLEM: Number of (Iobs-Icalc)/SigmaW > 10 Outliers ....          1 Check
RESPONSE: ...
;
_vrf_PLAT939_AFSCN
;
PROBLEM: Large Value of Not (SHELXL) Weight Optimized S .      12.50 Check
RESPONSE: ...
;
_vrf_PLAT971_AFSCN
;
PROBLEM: Check Calcd Resid. Dens.  2.00A   From S2             1.79 eA-3
RESPONSE: ...
;
_vrf_PLAT972_AFSCN
;
PROBLEM: Check Calcd Resid. Dens.  0.82A   From Au2           -1.70 eA-3
RESPONSE: ...
;
_vrf_PLAT978_AFSCN
;
PROBLEM: Number C-C Bonds with Positive Residual Density.          0 Info
RESPONSE: ...
;
# end Validation Reply Form
```

PLATON version of 17/03/2019; check.def file version of 04/03/2019

Datablock AFSCN - ellipsoid plot

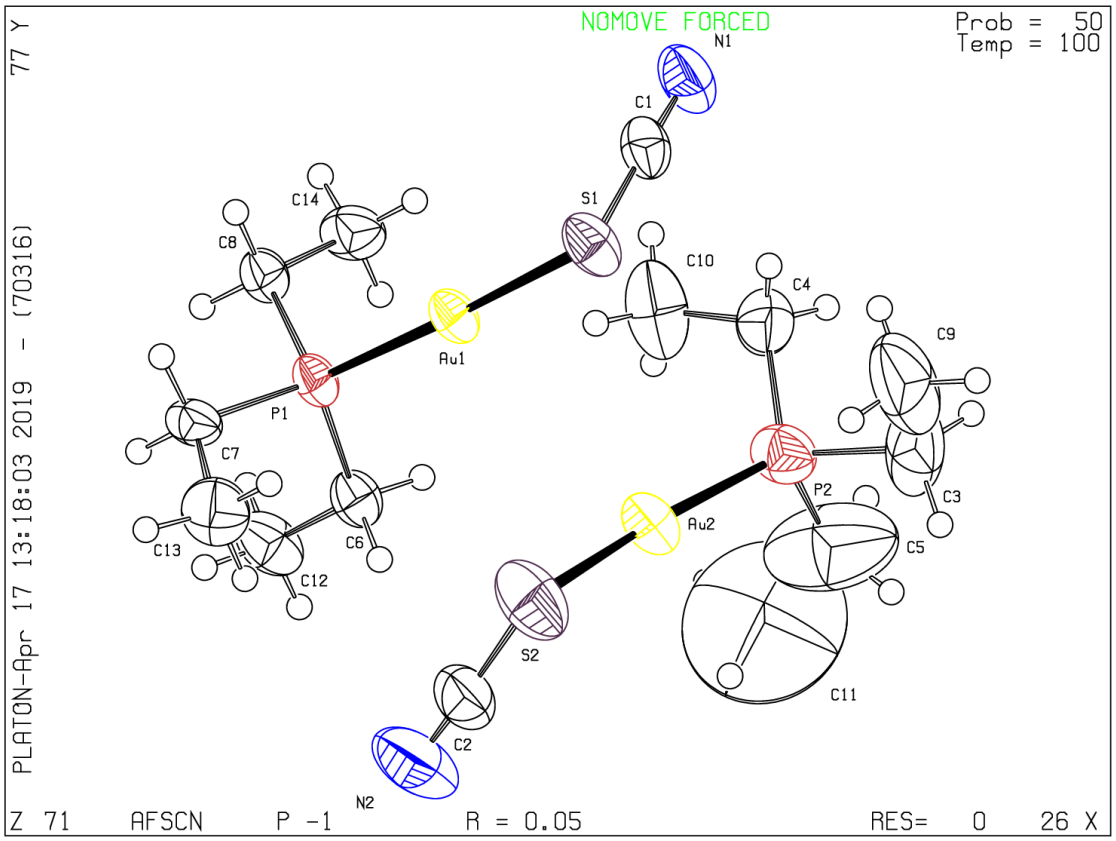

Structural and solution chemistry, antiproliferative effects, and serum albumin binding properties of three pseudohalide derivatives of Auranofin

SUPPORTING INFORMATION

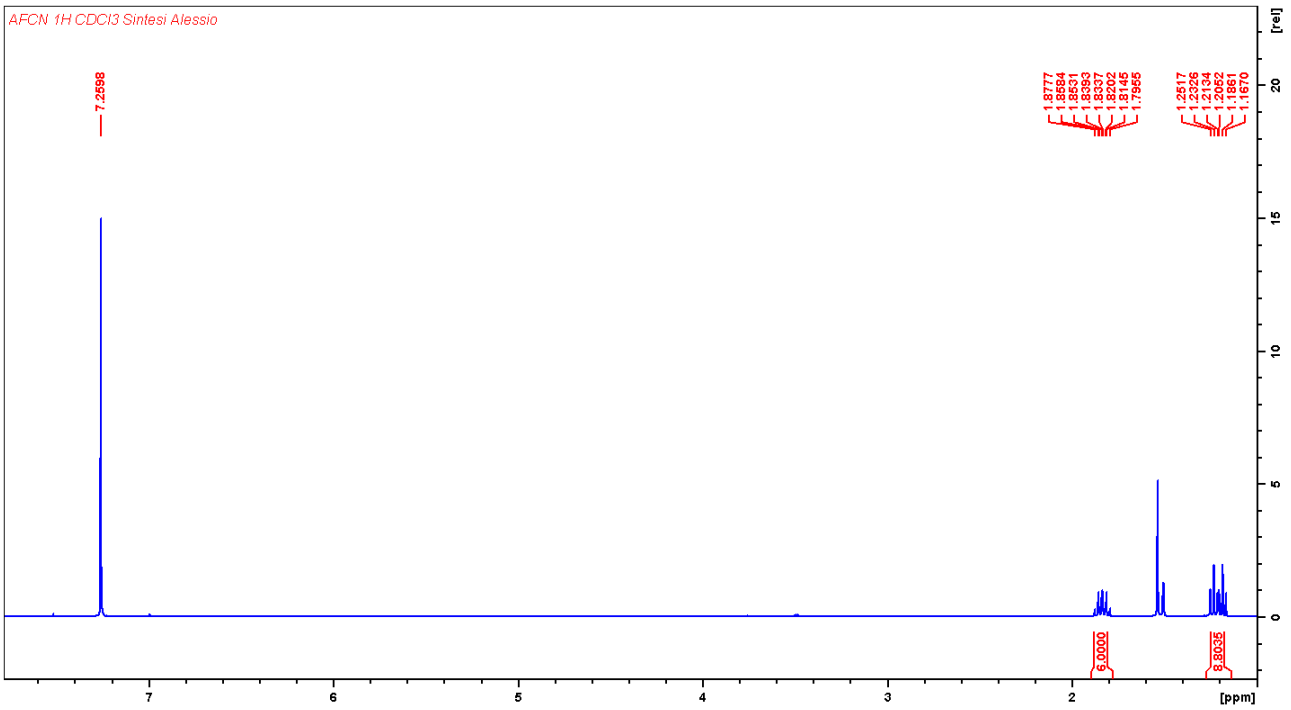

Fig.S1: ^{1}HNMR ($CDCl_3$; 400.13 MHz): 1.84 (dq; J_{HH} = 7.68 Hz; J_{PH} = 9.86 Hz; 6H); 1.21 (dt; J_{HH} = 7.65 Hz; J_{PH} = 18.59 Hz; 9H)

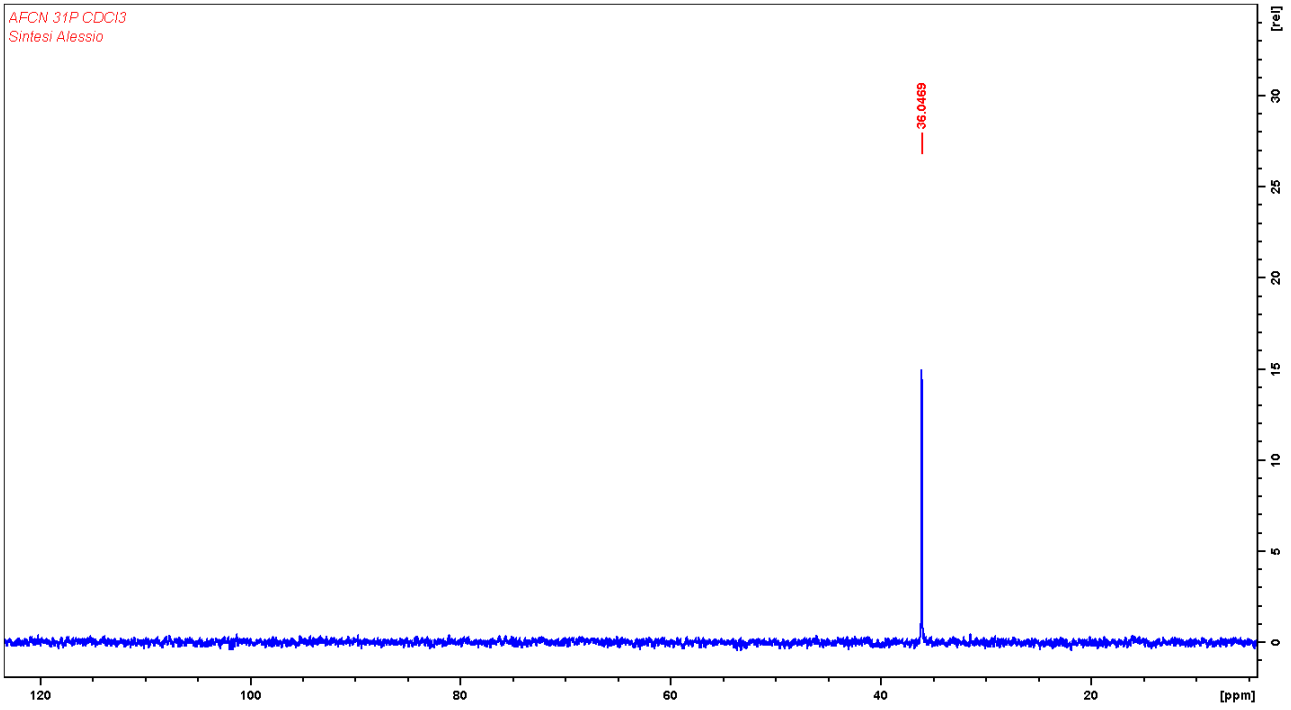

Fig.S2: ^{31}PNMR ($CDCl_3$; 161.98 MHz): 36.05

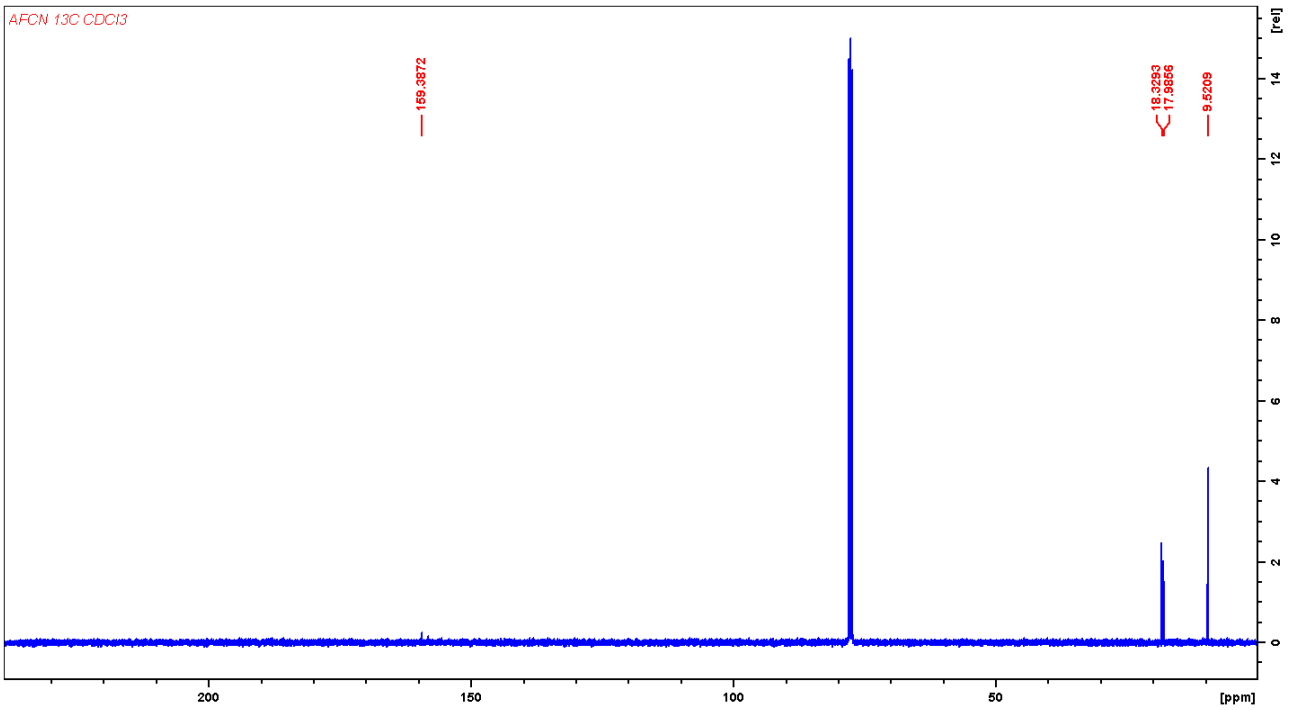

Fig.S3: ^{13}CNMR ($CDCl_3$; 100.61 MHz): 159.39; 18.16 (d; J_{CP} = 34.58 Hz); 9.52

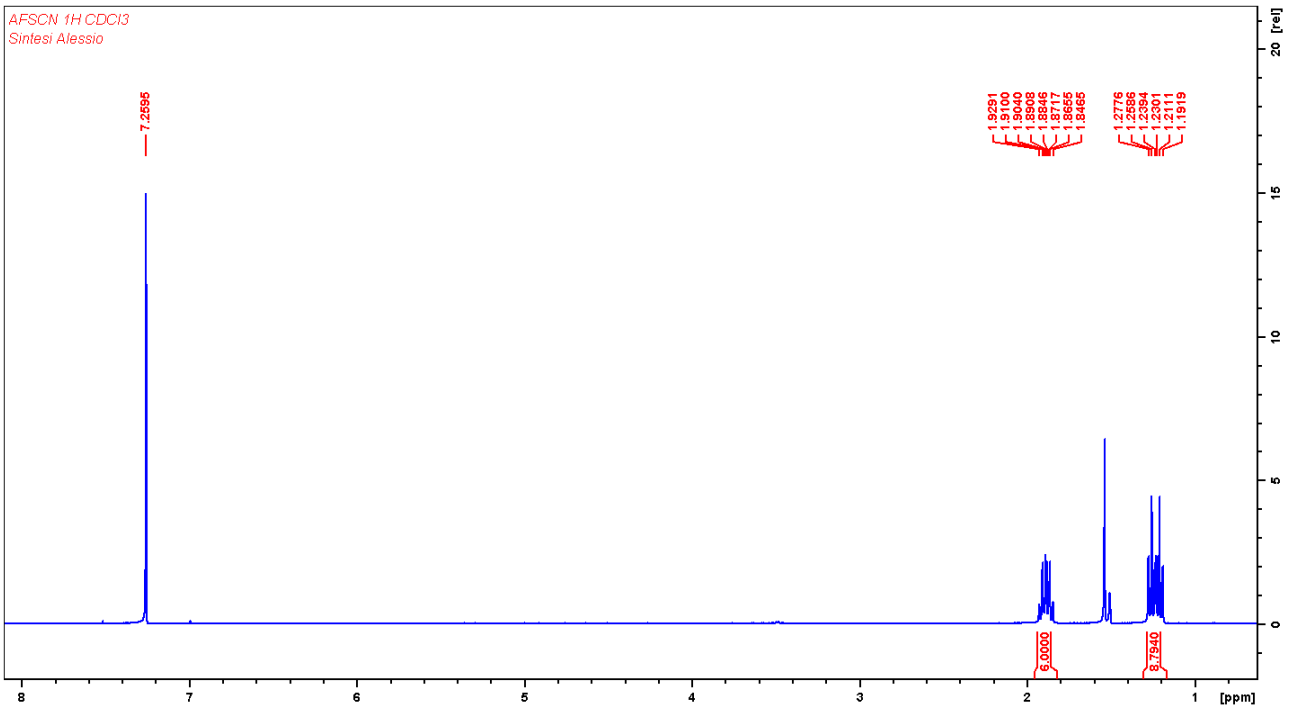

Fig.S4: ^{1}HNMR ($CDCl_3$; 400.13 MHz): 1.89 (dq; J_{HH} = 7.66 Hz; J_{PH} = 10.06 Hz; 6H); 1.23 (dt; J_{HH} = 7.64 Hz; J_{PH} = 19.00 Hz; 9H)

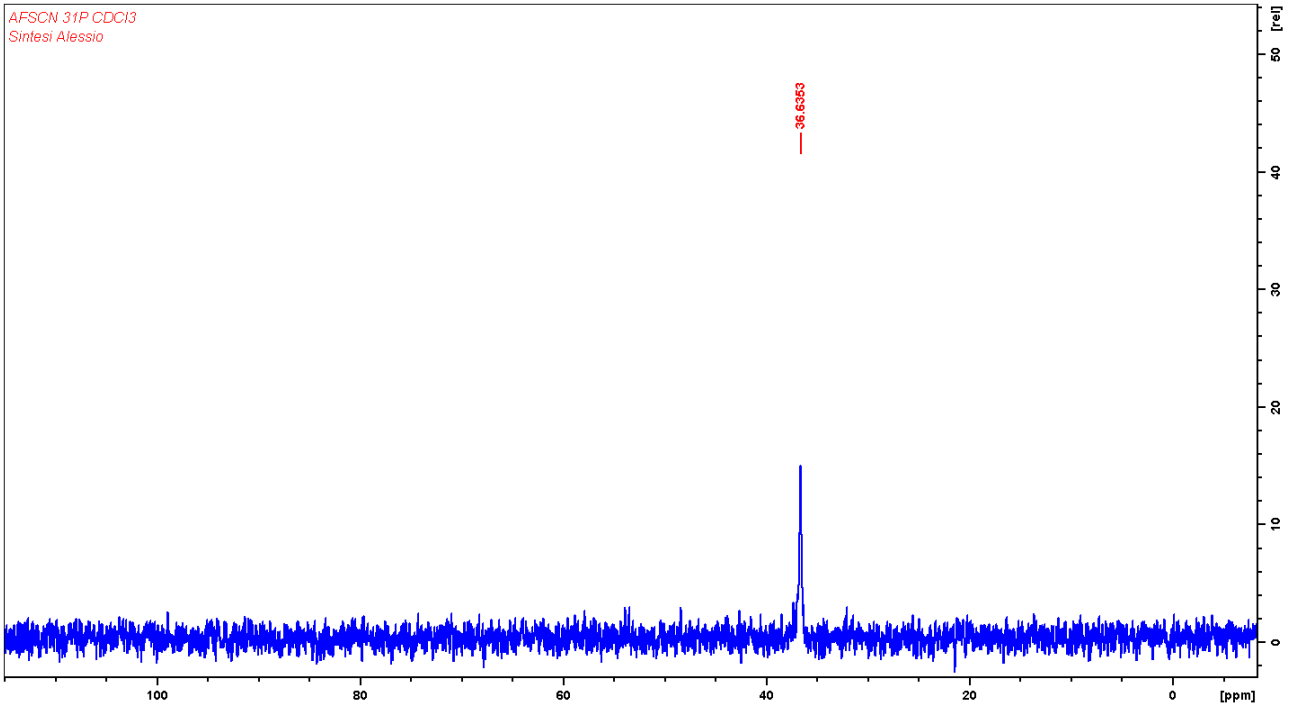

Fig.S5: ^{31}PNMR ($CDCl_3$; 161.98 MHz): 36.63

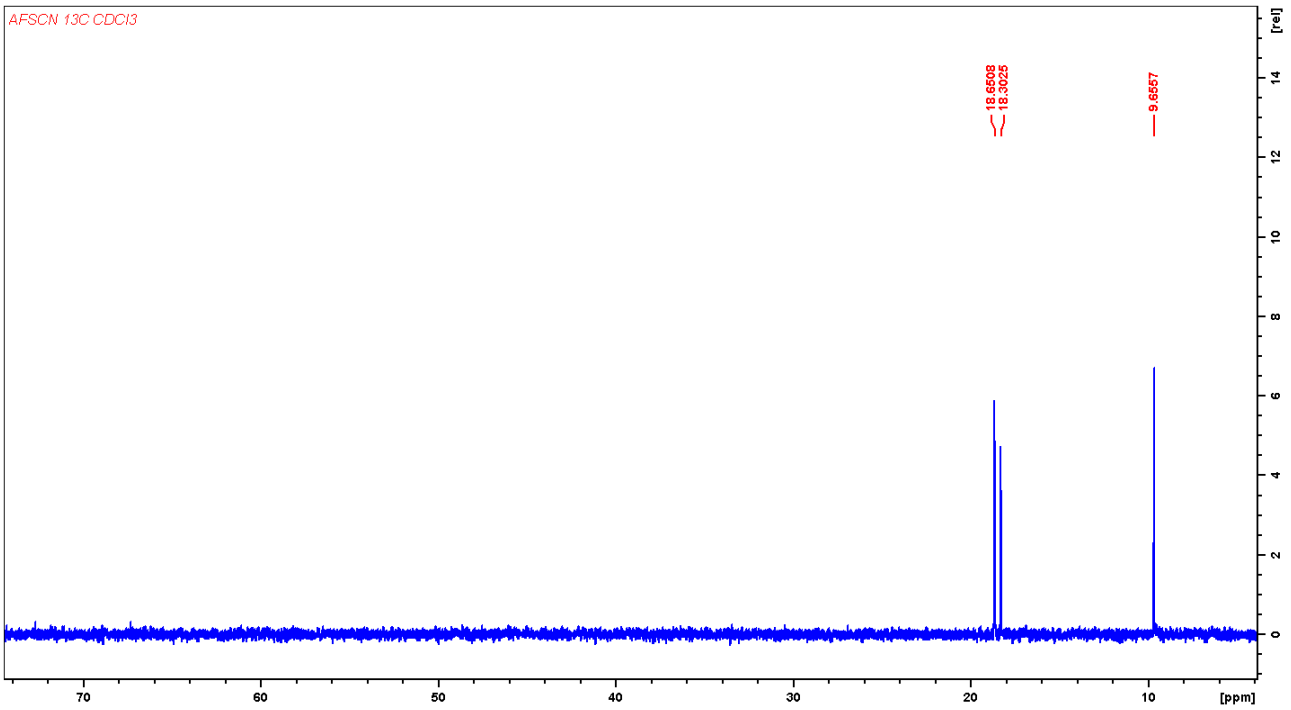

Fig.S6: ^{13}CNMR ($CDCl_3$; 100.61 MHz): 18.48 (d; J_{CP} = 35.04 Hz); 9.66

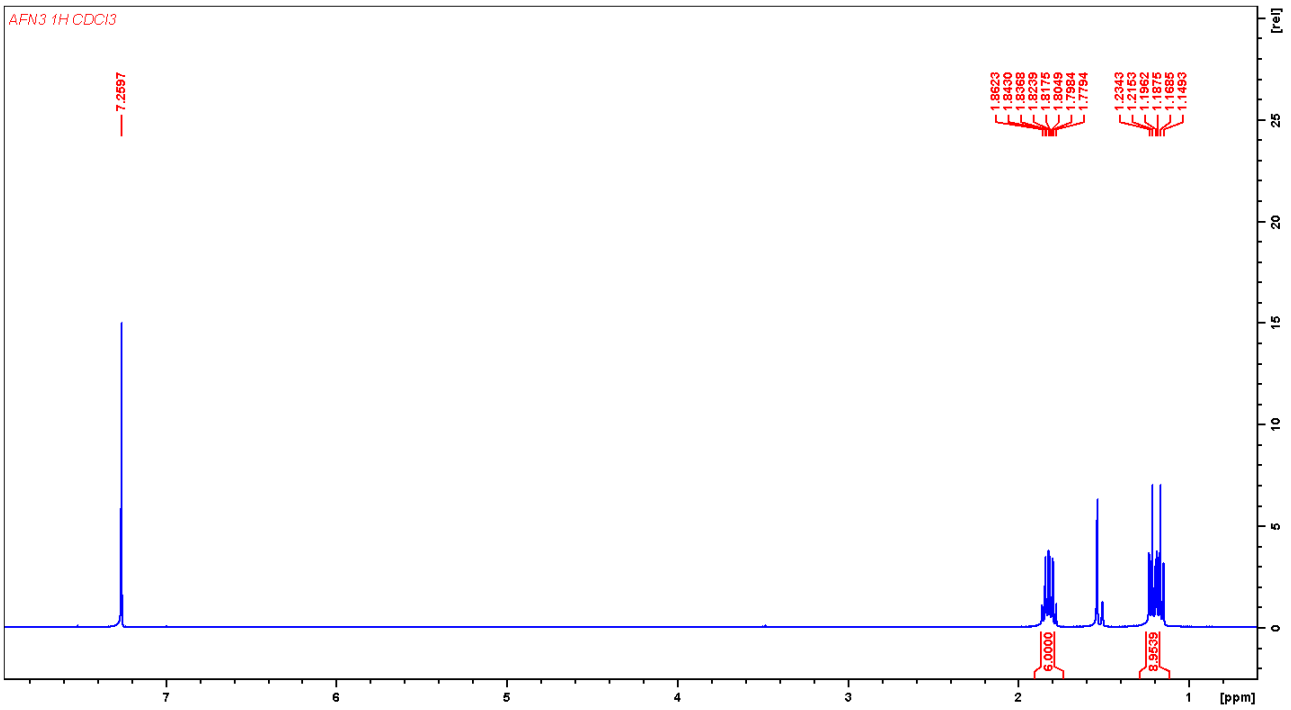

Fig.S7: ^{1}HNMR ($CDCl_3$; 400.13 MHz): 1.82 (dq; J_{HH} = 7.66 Hz; J_{PH} = 10.20 Hz; 6H); 1.19 (dt; J_{HH} = 7.63 Hz; J_{PH} = 18.75 Hz; 9H)

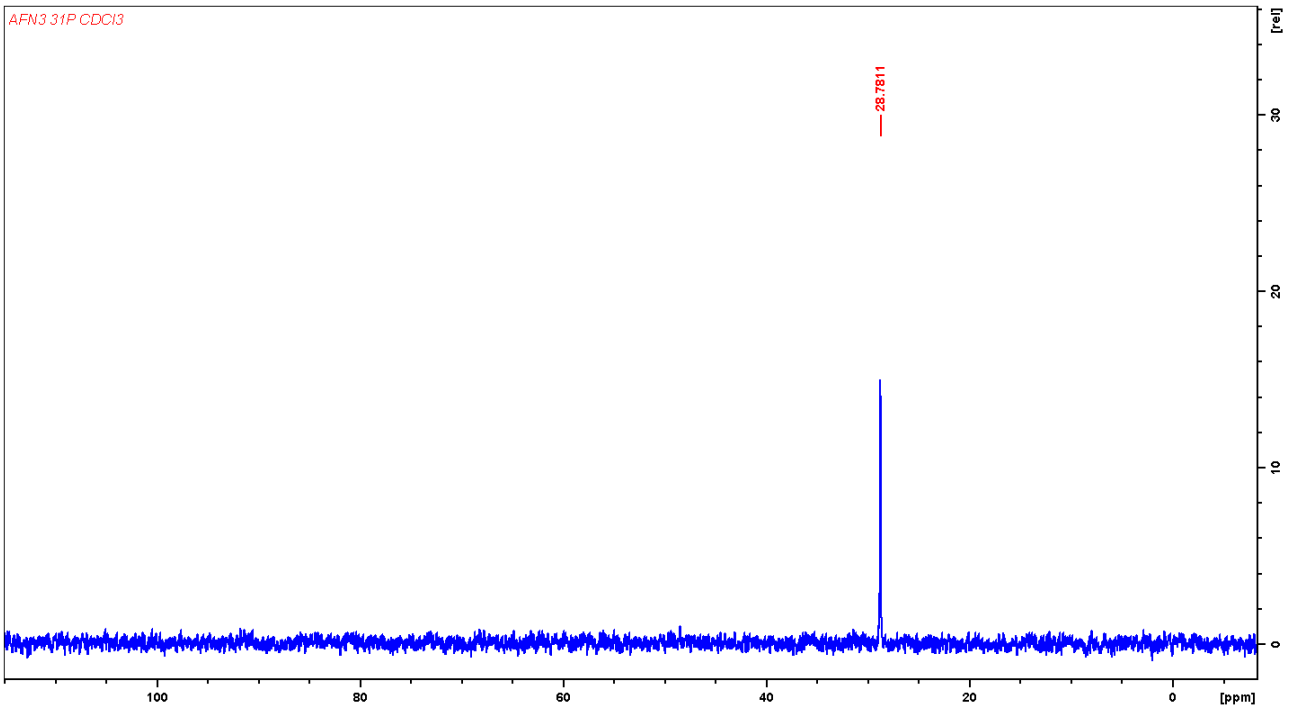

Fig.S8: ^{31}PNMR ($CDCl_3$; 161.98 MHz): 28.78

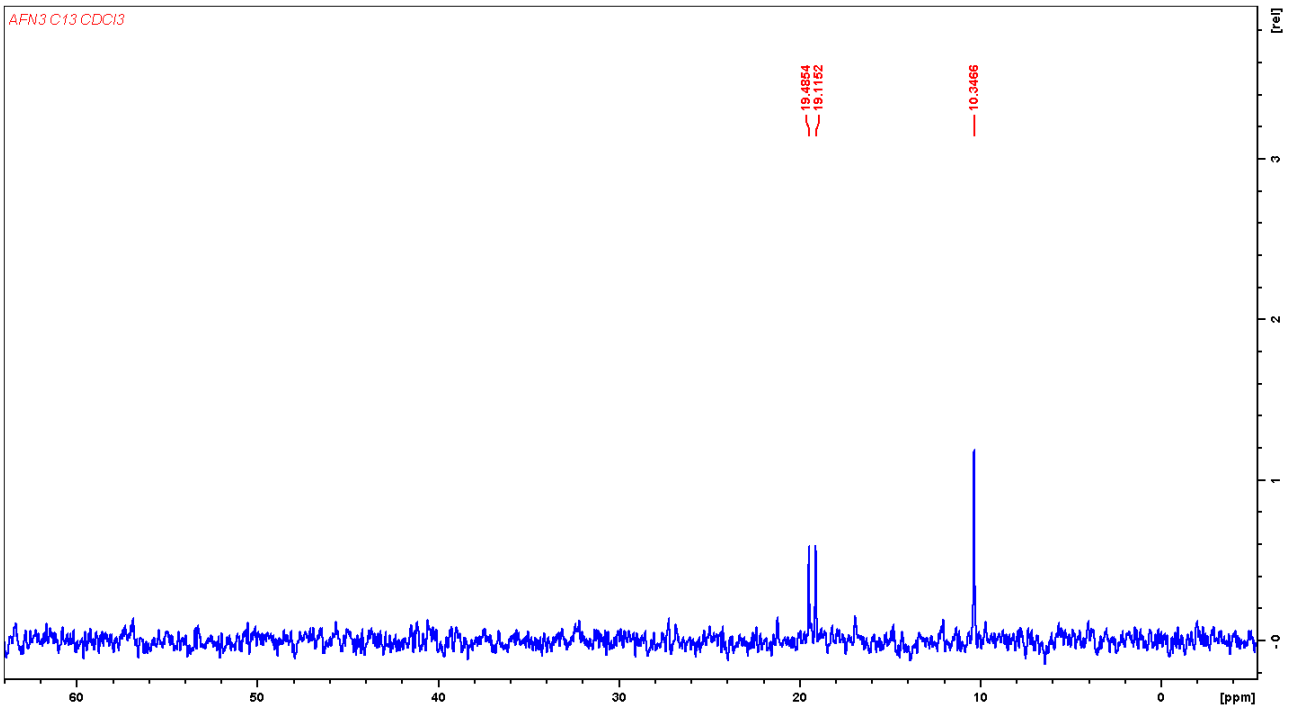

Fig.S9: ^{13}CNMR ($CDCl_3$; 100.61 MHz): 19.30 (d; J_{CP} = 37.25 Hz); 10.35

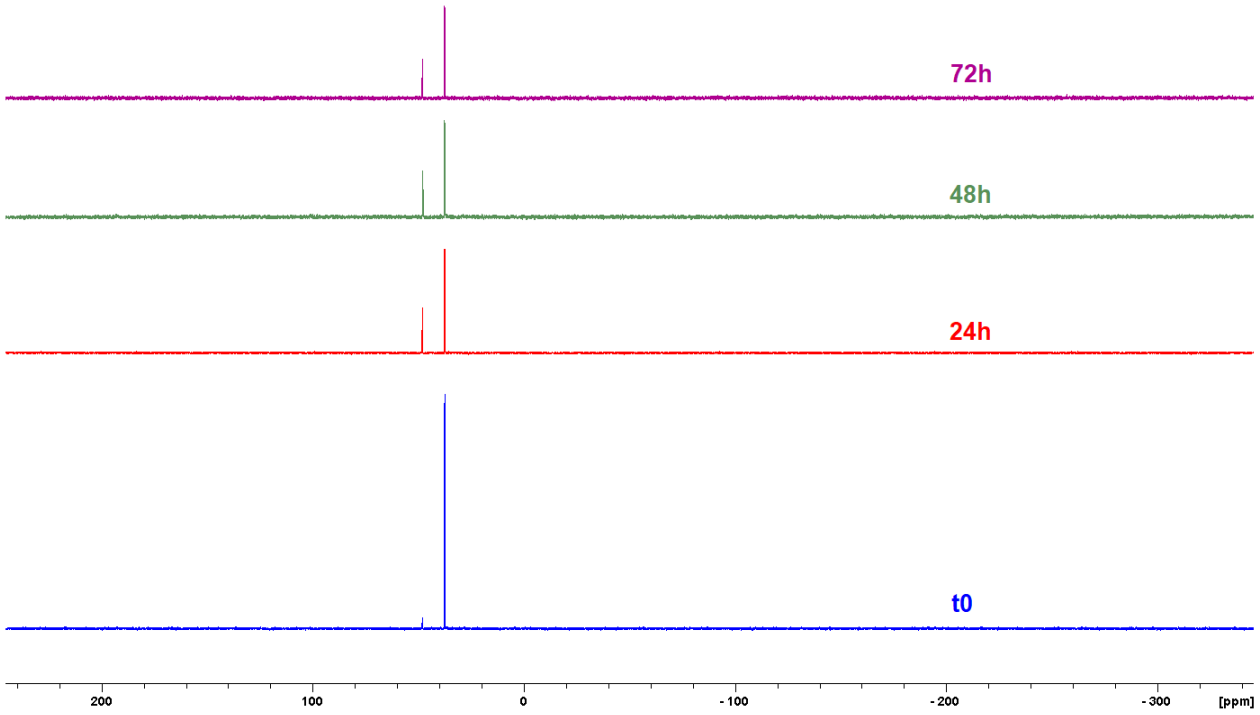

Fig.S10: AFCN stability in DMSO-d_6

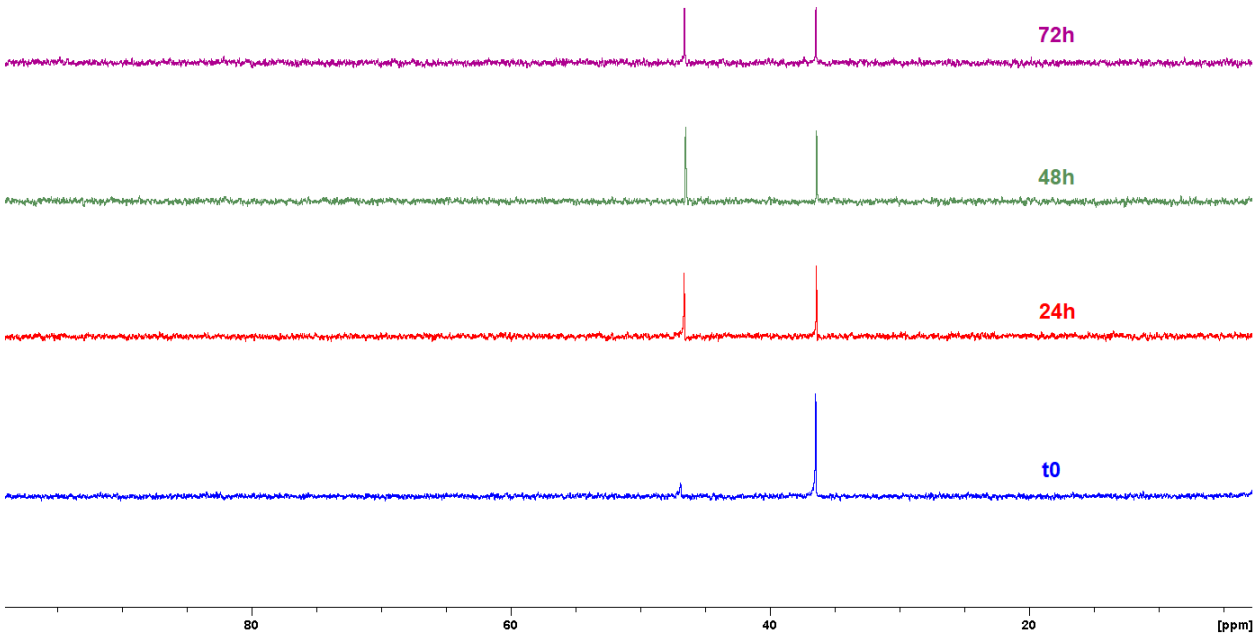

Fig.S11: AFCN stability in buffer phosphate (50mM pH 7.4) and DMSO-d_6 9:1

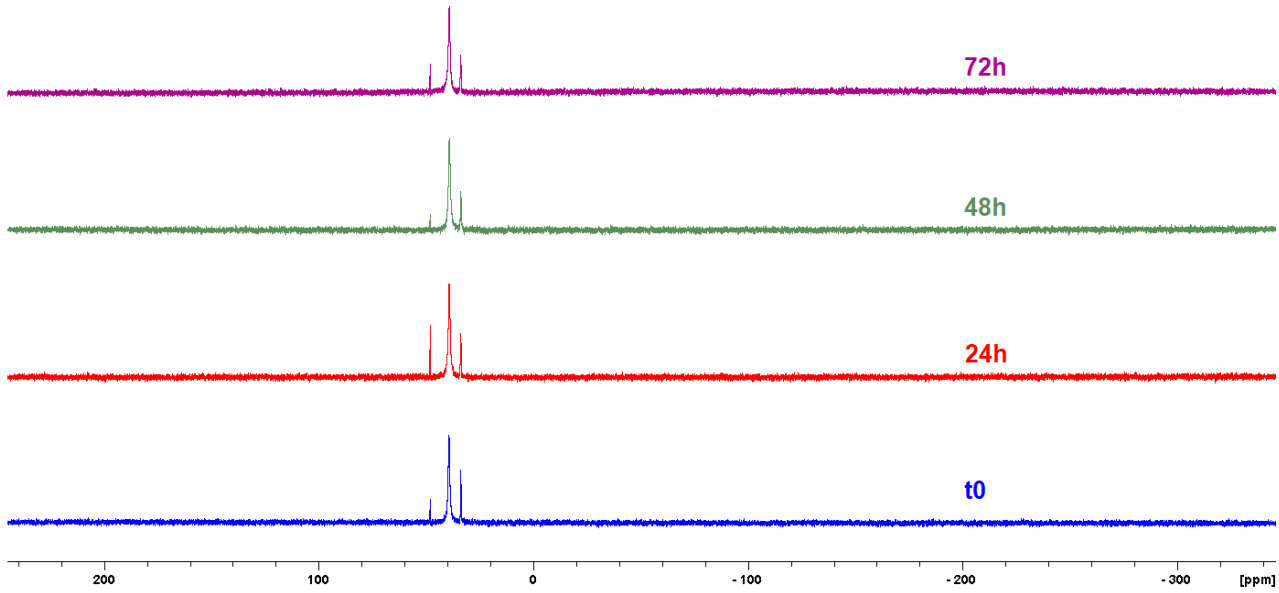

Fig.S12: AFSCN stability in DMSO-d_6

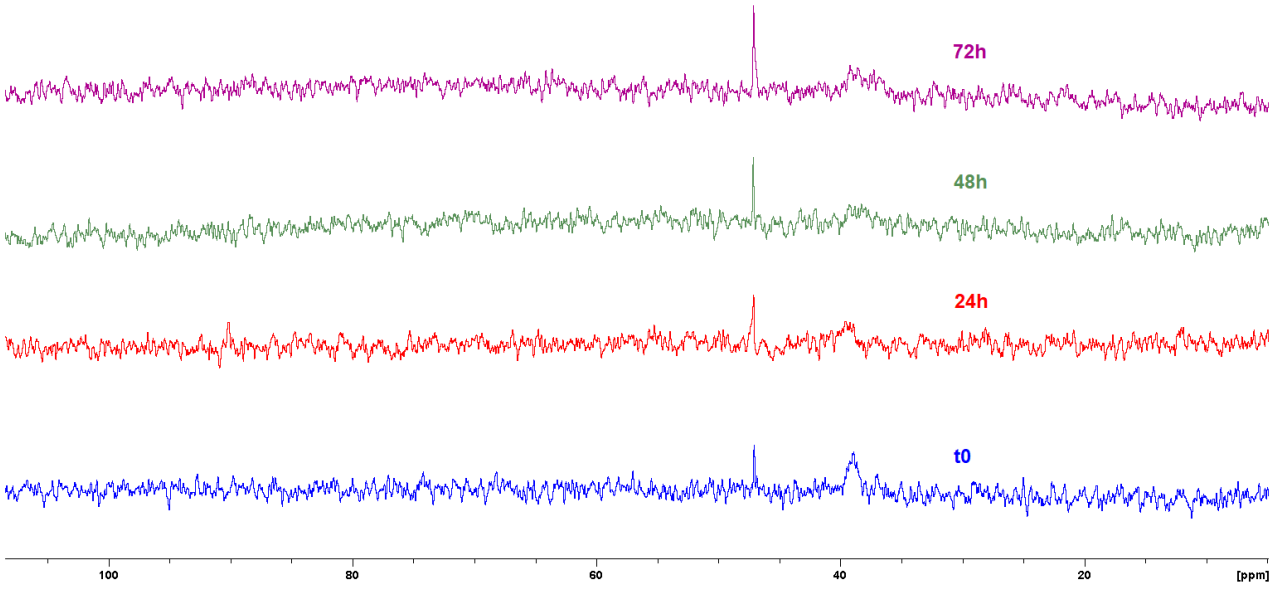

Fig.S13: AFSCN stability in buffer phosphate (50mM pH 7.4) and DMSO-d_6 9:1

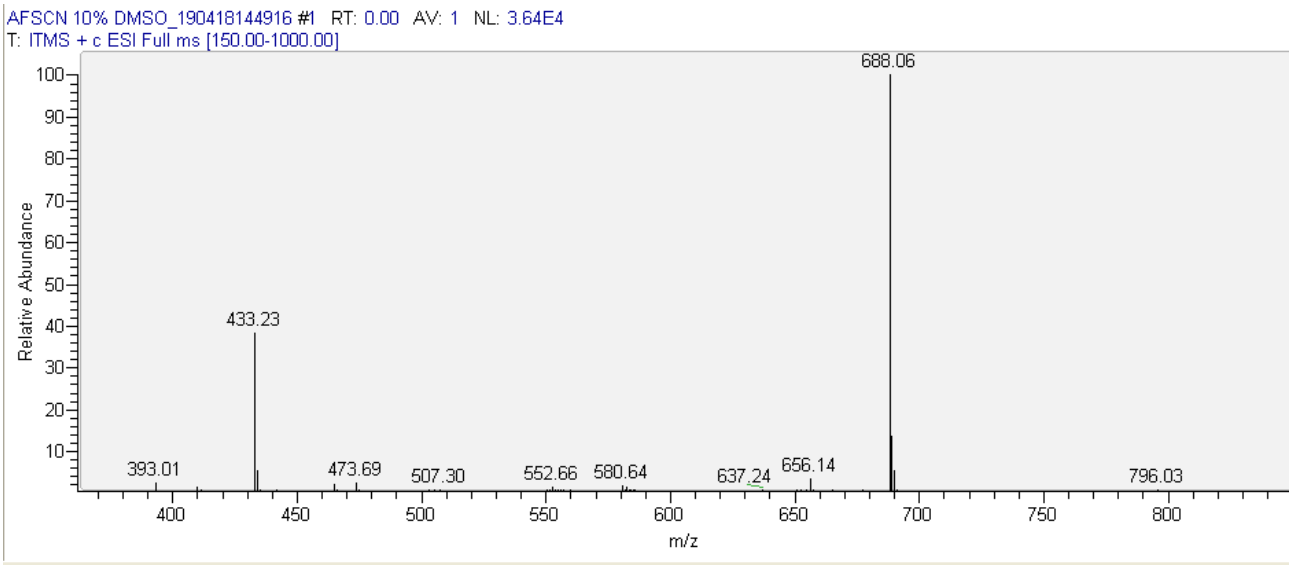

Fig.S14: ESI-MS spectra were recorded on a Thermo Fisher LCQ Fleet Ion Trap mass spectrometer. The sample was prepared after a dilution of 100 µL of solution $8*10^{-4}$ M of AFSCN in 900 µL of Hypergrade methanol for mass spectrometry.

The acquisition was carried in direct infusion. ESI-MS spectrum of AFSCN $8*10^{-5}$ M in MeOH/DMSO 9:1.

m/z: 393.01 $[Et_3PAuDMSO]^+$; 433.23 $[Au(PEt_3)_2]^+$; 688.06 $[Au_2(PEt_3)_2SCN]^+$

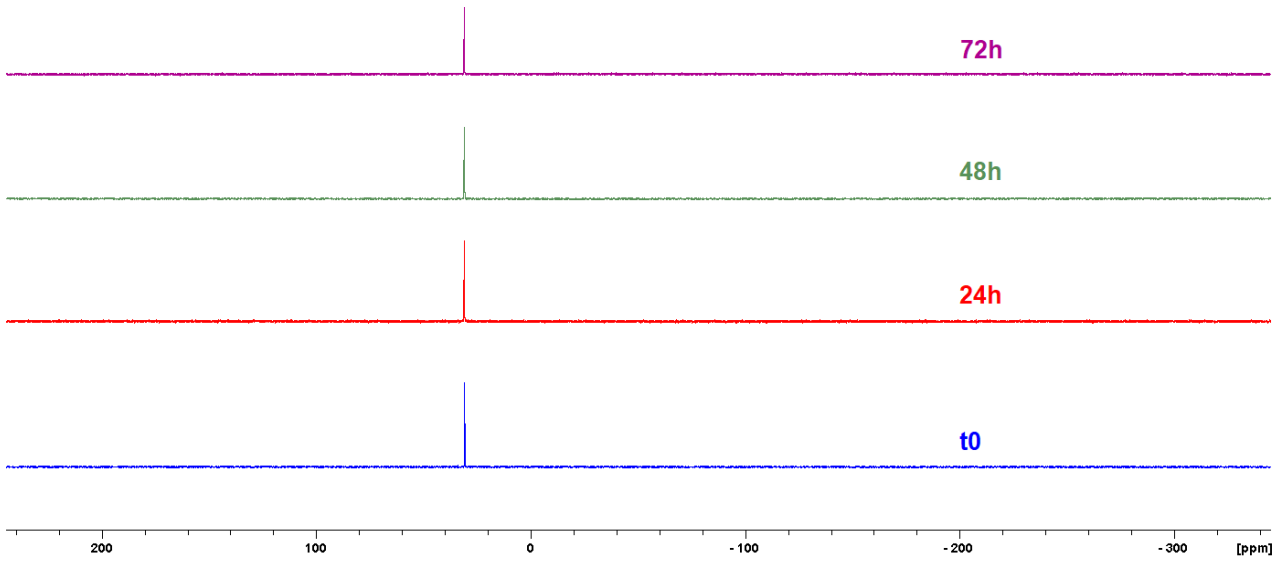

Fig.S15: AFN_3 stability in DMSO-d_6

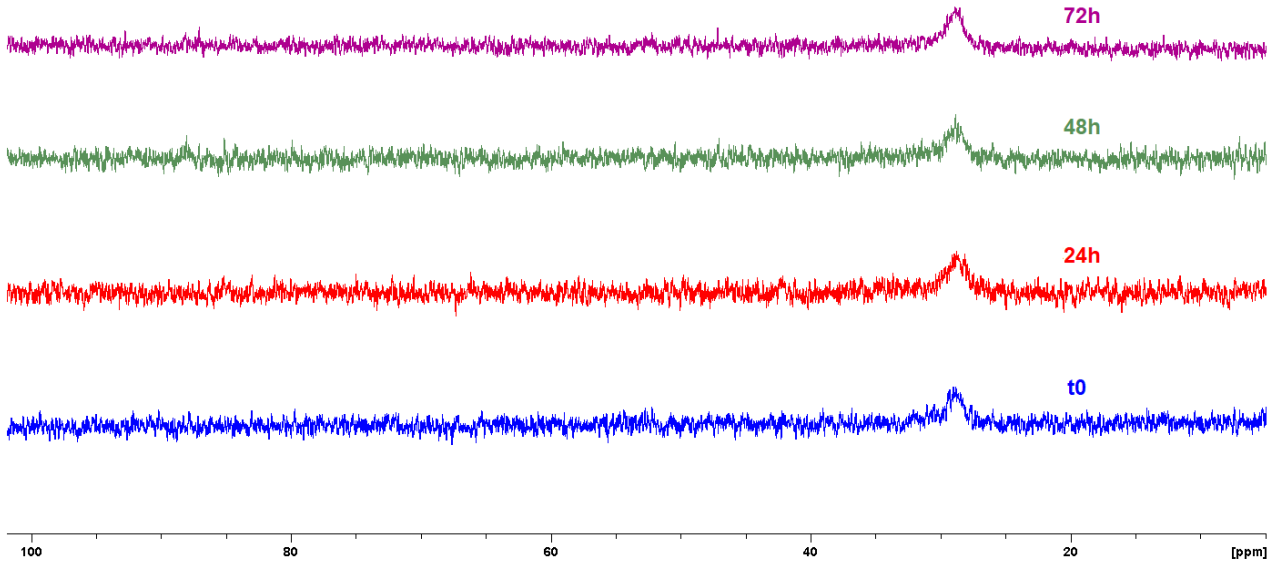

Fig.S16: AFN_3 stability in buffer phosphate (50mM pH 7.4) and DMSO-d_6 9:1

	AFSCN
Empirical formula	C14 H30 Au2 N2 P2 S2
Formula weight	746.39
Temperature (K)	100(2)
Wavelength (Å)	0.71073
Crystal system, space group	Triclino, P-1
Unit cell dimensions (Å)	a = 7.3651(7) α = 74.491(8) b = 12.0894(12) β= 83.768(8) c = 13.4821(12) γ = 78.215(8)
Volume ($Å^3$)	1130.50(19)
Z, D_c (mg/cm^3)	2, 2.193
μ (mm^{-1})	13.287
F(000)	696
Crystal size (mm)	0.2x0.04x0.03
θ range (°)	1.570 to 30.911
Reflections collected / unique	6287/3953
Data / restraints / parameters	3953/ 3 / 199
Goodness-of-fit on F^2	1.064
Final R indices [I>2σ(I)]	R1 = 0.0511, wR2 = 0.0958
R indices (all data)	R1 = 0.0988, wR2 = 0.1372

Table S1: Crystal data and refinement parameters for X

	AFSCN
Au(1)–P(1)	2.260(2)
Au(1)–S(1)	2.330(2)
Au(2)–P(2)	2.251(3)
Au(2)–S(2)	2.320(3)
P(1)–Au(1)–S(1)	177.61(11)
P(2)–Au(2)–S(2)	172.78(14)
Au(1)–S(1)–C(1)	100.1(3)
Au(2)–S(2)–C(2)	103.6(5)

Table S2: Bond lengths (Å) and angles (°) for compound AFSCN

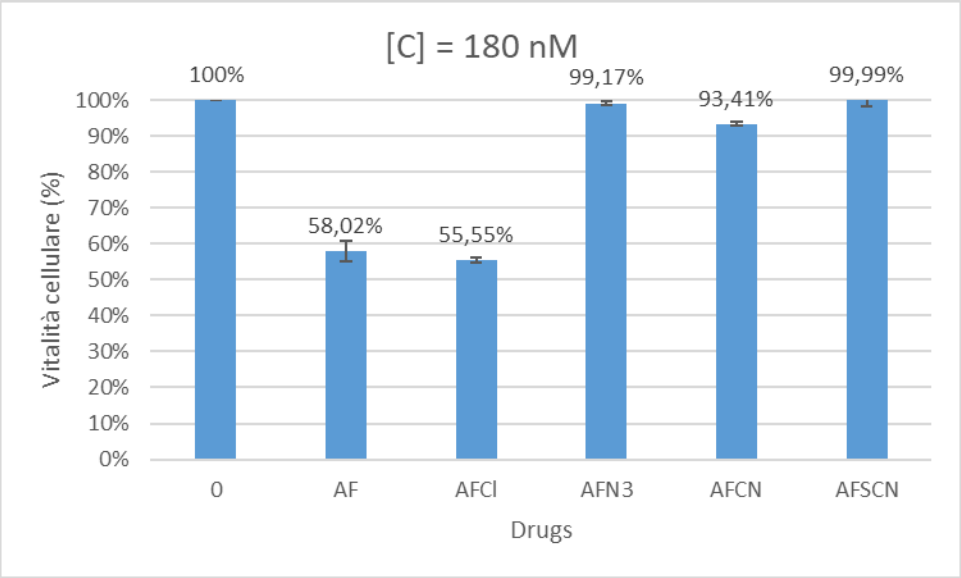

Fig.S23: Comparison between Auranofin and Et_3PAuCl and the three studied compounds against HCT116 cell line at 180 nM

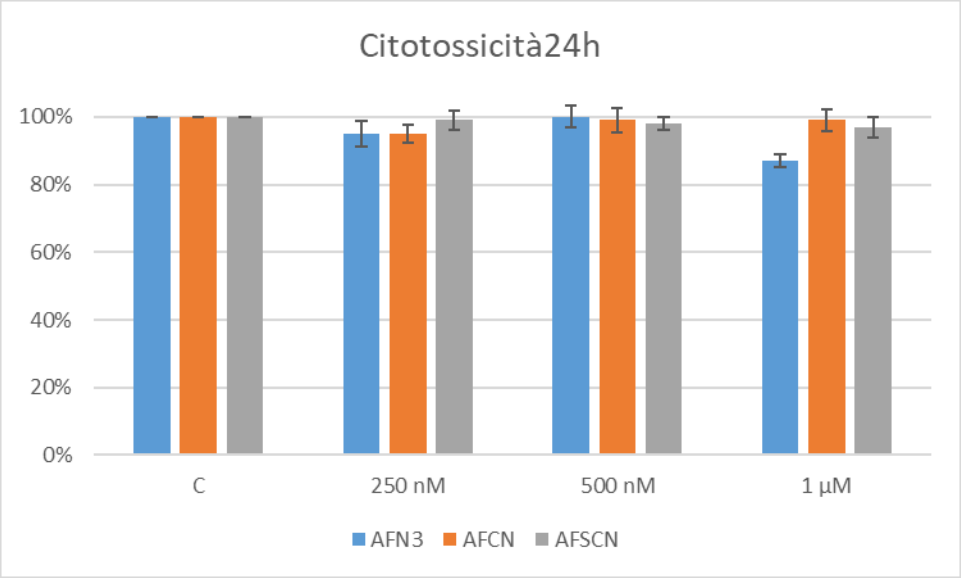

Fig.S24: The three investigated compounds tested at concentrations up to 1 µM on HCT116 cell line

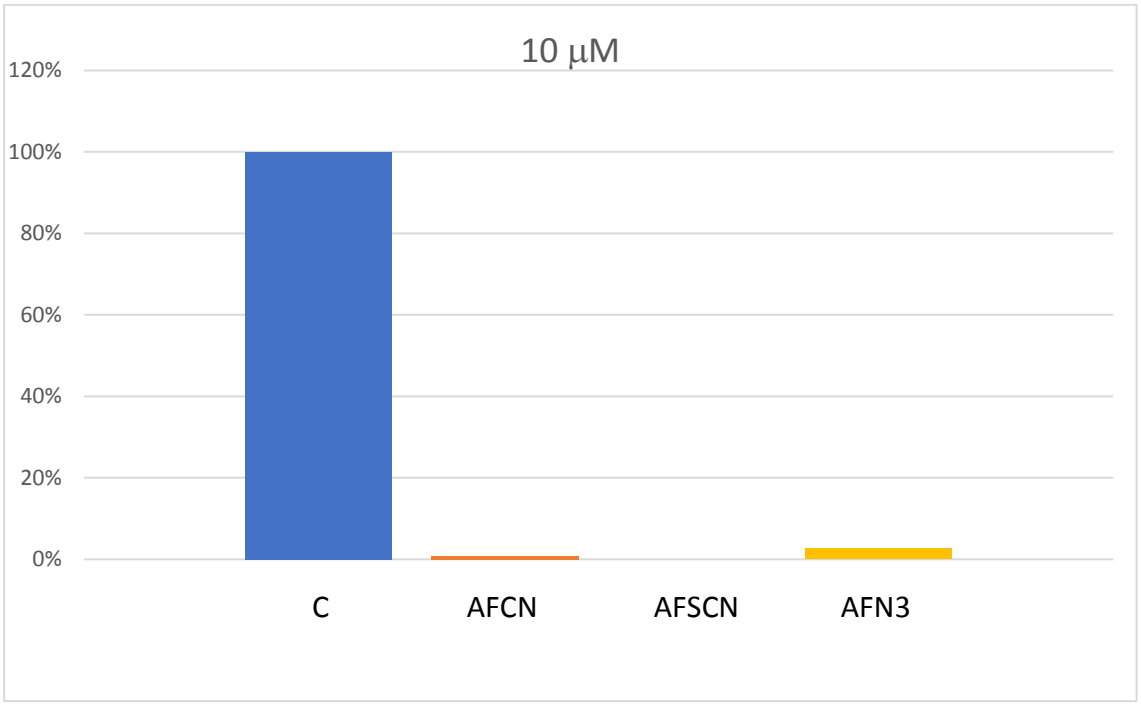

Fig.S25: The three investigated compounds tested at 10 μM on HCT116 cell line